Electronic Supplementary Material (ESI) for Dalton Transactions.
This journal is © The Royal Society of Chemistry 2023

UV Induced Hydrophosphination of Dimethyl 2-Vinylcyclopropane-1, 1-Dicarboxylate Towards Phosphine Chalcogenides

Supporting Information

Jeanette A. Adjei, Michael A. Kerr*, Paul J. Ragogna*

The University of Western Ontario, Department of Chemistry,

London, Ontario, Canada N6A 5B7

Correspondence email: makerr@uwo.ca, pragogna@uwo.ca

Table of Contents

Sample Calculations for NMR Conversion Determined with An Internal Standard S-2
Optimization Table for the Synthesis of **4a** & **5a** S-5
Control Reactions S-7
UV-Vis Spectrum of **1b**, **3** & Mixture of **1b** + **3** S-11
Spectra and High-Resolution Mass Spectrometry of Control Reactions S-13
NMR Characterization of Phosphines, Phosphine Sulfides and Phosphine Oxide S-22
Crystallographic information S-49
References S-53

Sample Calculations for NMR Conversion Determined with An Internal Standard

0.078 g of ferrocene was dissolved in 2 mL of $CDCl_3$ to obtain a 0.21 M solution. 60 µL of the ferrocene solution was charged to a capillary tube and the end of the tube was sealed with a butane flame torch. 0.115 g of triphenylphosphine was dissolved in 2 mL of $CDCl_3$ to obtain a 0.22 M solution. 60 µL of the triphenylphosphine was charged to a capillary tube and the end of the tube was sealed. These standards were used to determine the NMR conversion using ^{1}H and $^{31}P\{^{1}H\}$ NMR spectroscopy respectively.

4a: The signals belonging to PPh_3 and compound **4a** were integrated and NMR conversion was obtained.

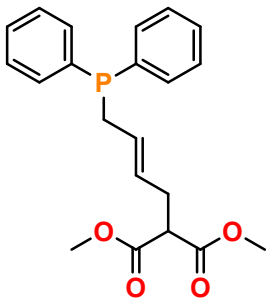

A

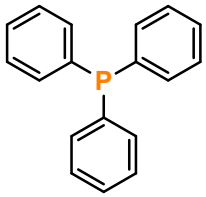

IS

N = number of nuclei

Ratio of the integrals: $r_{A/IS} = \frac{n_A}{n_{IS}} = \frac{(integral_A/N_A)}{(integral_B/N_{IS})}$

$$r_{A/B} = \frac{n_A}{n_{IS}} = \frac{(10.13/1)}{(1/1)} = 10.13$$

$$n_{Is} = 0.00006\ L \times 0.22\ M = 0.0000132\ mol = 0.0132\ mmol$$

$n_A = n_{IS} \times r_{A/B} = 0.0132$ mmol x 10.13 = 0.133716 mmol

Compound **3** is the limiting reagent: mol: $\frac{0.0577\ g}{184.19\ g/mol} = 0.00031326\ mol = 0.31326\ mmol$

Theoretically yield is 0.31326 mmol

NMR conversion was:

$$A = \frac{0.133716\ mmol}{0.31326\ mmol} = 43\%$$

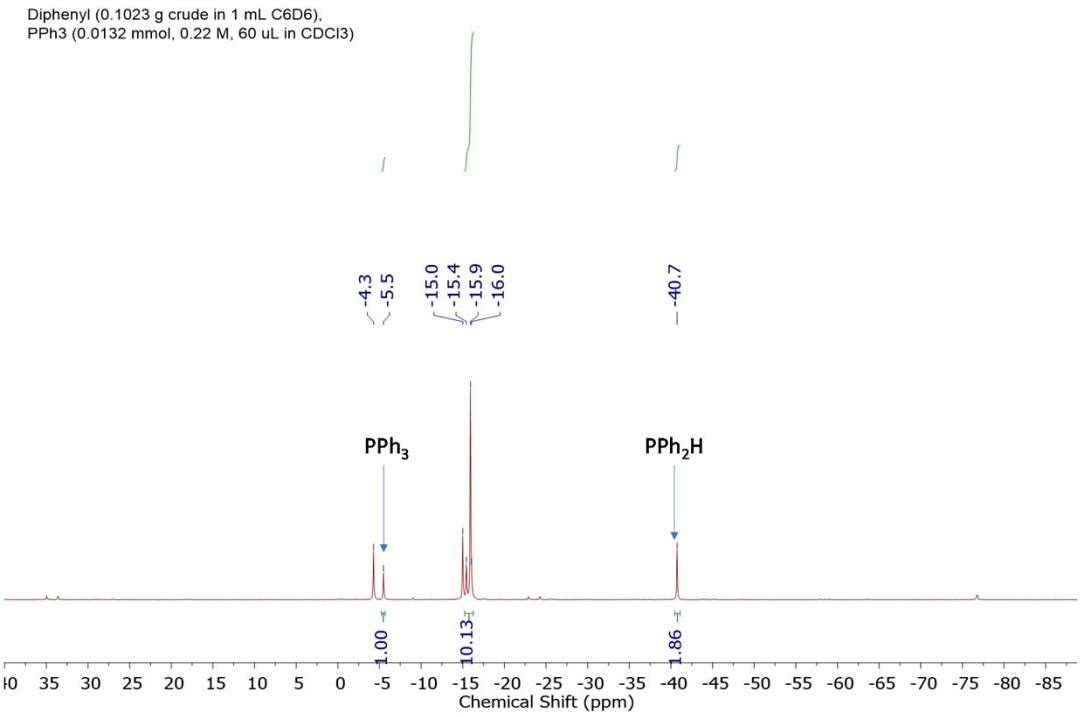

Figure S 1: $^{31}P\{^{1}H\}$ NMR spectrum of 4a. recorded in C_6D_6. NMR conversion was determined using PPh_3 as an internal standard. 43% of compound 4a was present in the crude material. This spectrum was used to demonstrate the sample calculation (above).

5c: Signals which belonged to A and B present in ^{1}H NMR spectrum were integrated, and the NMR conversion was obtained.

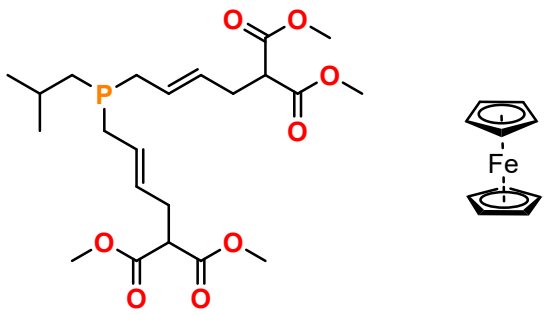

A **IS**

N = number of nuclei

Ratio of the integrals: $r_{A/IS} = \frac{n_A}{n_{IS}} = \frac{(integral_A/N_A)}{(integral_B/N_{IS})}$

$$r_{A/B} = \frac{n_A}{n_{IS}} = \frac{(6.43/6)}{(1/10)} = \frac{1.07166667}{0.1} = 10.7166667$$

$$n_{Is} = 0.00006\ L \times 0.21\ M = 0.0000126\ mol = 0.0126\ mmol$$

$n_A = n_{IS} \times r_{A/B} = 0.0126$ mmol x 10.7166667 = 0.13503 mmol

Compound **2c** is the limiting reagent: mol: $\frac{0.0549\ g}{90.11\ g/mol} = 0.00060926\ mol = 0.60925\ mmol$

Theoretically yield is 0.60925 mmol

NMR conversion was:

$$A = \frac{0.13503\ mmol}{0.60925\ mmol} = 22\%$$

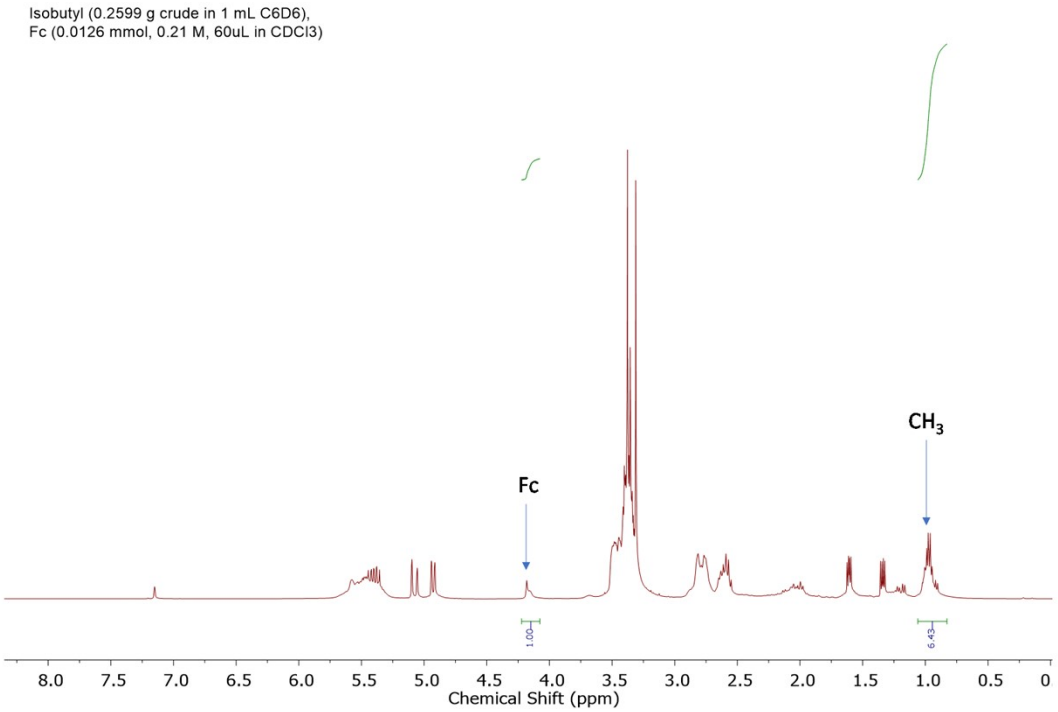

Figure S 2: ^{1}H NMR spectrum of isolated 5c recorded in C_6D_6.

NMR conversion for compound **5a**: 54% (0.2572 g crude in 1 mL of C_6D_6 phenyl protons were integrated), **5b**: 63% (0.2700 g crude in 1 mL of C_6D_6, olefin protons were integrated), **5d**: 51% (0.1736 g crude in 1 mL of C_6D_6, phenyl protons were integrated).

Optimization Table for the Synthesis of **4a** & **5a**

Different solvents (toluene, diethyl ether, benzene, DCM, MeCN) were used for P-H bond addition. There were signs of conversion, however THF became the solvent of choice for these reactions. Unless otherwise stated the reactions were performed at a 50 mg scale in borosilicate NMR tubes. There were inconsistencies in the results when 1.1 equiv. of **1a** was used. As a result, 1.5 equiv. of **1a** were used to ensure consistent results. For the optimization of **5a**, consistent results were obtained when 2.55 equiv. of cyclopropane **3** was used.

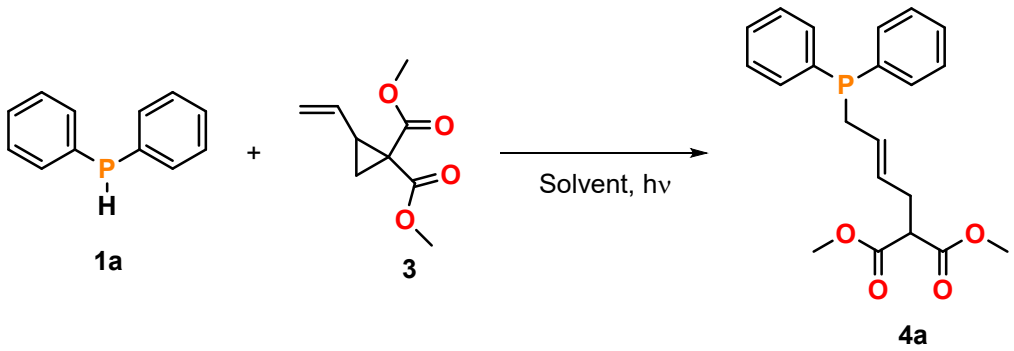

Table S 1: Reaction conditions for the optimization of 4a

Entry	Equivalents of **1a**	**3**	Time (h)	Results
1[ab]	1.1	1	4	Mixture of **1a** & **3**, **4**
2[cd]	1.1	1	9	Full conversion of **3**. **1a** present
3[e]	1.5	1	8	Full conversion of **3**. **1a** present
4[d]	1.5	1	8	Full conversion of **3** **1a** present
5[df]	1.1	1	2	**3** (7%), **4a** (86%) & **1a**[g]
6[df]	1	1	3	**3** (9%), **4a** (85%) & **1a**[g]
7[df]	1.5	1	2	**1a** (28%) & **4a** (58%)[h]

[a]Entries were preliminary trials, there was a focus on qualitative results rather than quantitative results. [b]C_6D_6 was used as a solvent. [c]250 mg scale reaction. [d]THF was used as a solvent. [e]Toluene was used as a solvent. [f]Reaction vessel was a quartz NMR tube. [g]NMR conversion were obtained *via* ^{1}H NMR integration. [h]NMR conversion were obtained from $^{31}P\{^1H\}$ NMR integration.

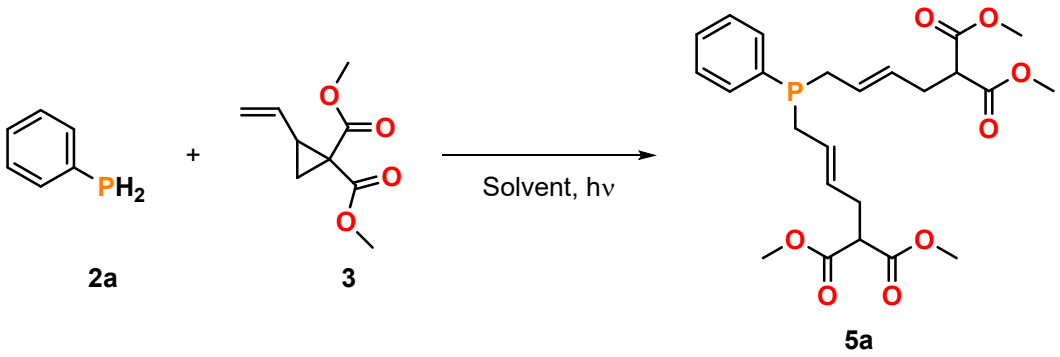

Table S 2: Reaction conditions for the optimization of 5a

Entry	**2a**	Equivalents of **3**	Time (h)	Results
1[a]	1	2	2	Mixture of 2° phosphine, **5a** & impurities. Full conversion of **3**.
2[b]	1	2.4	2.5	Full conversion of **3**. Mixture of 2° phosphine & **5a**.
3[b]	1	2.5	3	Mixture of **3** and **5a** present (0.05:4)[c]
4[b]	1	2.55	2.5	Mixture of **3** and **5a** present (0.25:4)[c]
5[b]	1	2.6	2.5	Mixture of **3** and **5a** present (0.21:4)[c]
6[b]	1	2.8	2.5	Mixture of **3** and **5a** present (0.12:4)[c]
7[b]	1	3	2	Mixture of **3** and **5a** present (0.55:4)[c]
8[de]	1	2.55	2	**5a** (99%), **3** (14%)[f]

[a]Toluene was used as a solvent. [b]C_6D_6 was used as a solvent. [c]The ratio of **3** and **5a** was determined *via* ^{1}H NMR spectroscopy. [d]THF was used as a solvent. [e]Reaction vessel was a quartz NMR tube. [f]NMR conversions were obtained *via* ^{1}H NMR integration.

Control Reactions

General procedure for control reactions

In a nitrogen filled glovebox, cyclopropane **3** (0.05 g, 0.2714 mmol, 1 equiv.), **1b** (0.04 g, 47 µL, 0.4072 mmol, 1.5 equiv.) and distilled THF (0.9 mL, 0.3 M) were charged into a quartz NMR tube. The reaction solution was irradiated with UV light for 8 h. The volatiles were removed in *vacuo* and an oil was recovered. The ^{1}H and $^{31}P\{^{1}H\}$ NMR spectra and HRMS were recorded.

The same procedure was used when 1-hexene was treated with **1b**. The reactions were performed in a quartz NMR tube or a tube, the solutions were irradiated with UV light.

TEMPO: (2,2,6,6-Tetramethylpiperidin-1-yl)oxy, BHT: Butylated hydroxytoluene, DPE: 1,1-Diphenylethylene

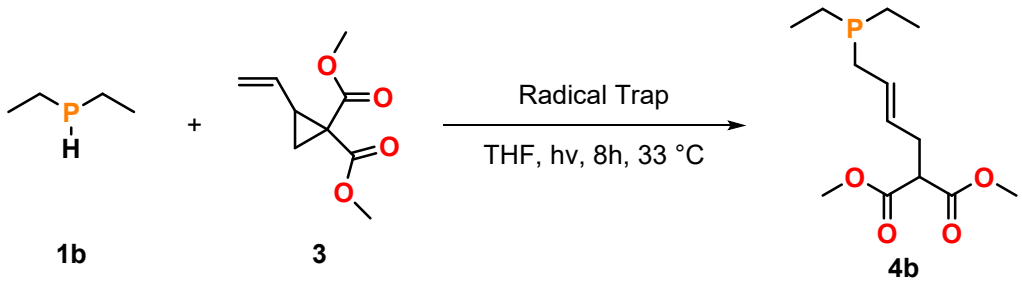

Table S 3: Control Reactions

Entry	Radical Trap	Condition	Results
1	None	Dark, r.t., overnight	No reaction
2	None	75 °C, overnight	No reaction
3	None	1 mol% of AIBN, 75 °C, overnight	Formation of **4b**
4	None	hv, 9h	Formation of tetraethyldiphosphine
5	None	hv, 8h	Decomposition
6	TEMPO (1 equiv.)	hv	No formation of **4b**
7	BHT (1 equiv.)	hv	Full NMR conversion of **3**
8	DPE (1 equiv.)	hv	0% isolated yield
9	TEMPO (10 mol%)	hv	Full NMR conversion of **3**

10	BHT (10 mol%)	hv	Full NMR conversion of **3**
11	DPE (10 mol%)	hv	Mixture of VCP and **4b**
12	None	1 equiv. of 1-hexene was used as an olefin	30% isolated yield
13	None	1-hexene, 15 mL quartz tube was used as a reaction vessel	32% isolated yield
14	None	UV solution filter: 1.77 M aqueous solution of $NiSO_4 \cdot H_2O$, 0.29 M aqueous solution of $CoSO_4 \cdot H_2O$ and 1.16 x 10^{-4} M of 1,4 diphenyl butadiene in diethyl ether	87% isolated yield

TEMPO (1 equiv.) – No formation of product, HRMS detected phosphine-TEMPO adduct but there was a -6.5 ppm mass error.

BHT (1 equiv.) – There was full conversion of reactant to product, HRMS detected an inaccurate mass of the phosphine-BHT adduct.

DPE (1 equiv.) – No formation of product, HRMS detected phosphine-DPE adduct with good accuracy.

TEMPO (10 mol%) – Full conversion to product, HRMS detected phosphine-TEMPO adduct but there was a 11.1 ppm mass error.

BHT (10 mol%) – Full conversion to product, HRMS detected an inaccurate mass of the phosphine-BHT adduct.

DPE (10 mol%) – Mixture of **3** and product, HRMS detected phosphine-DPE adduct with good accuracy.

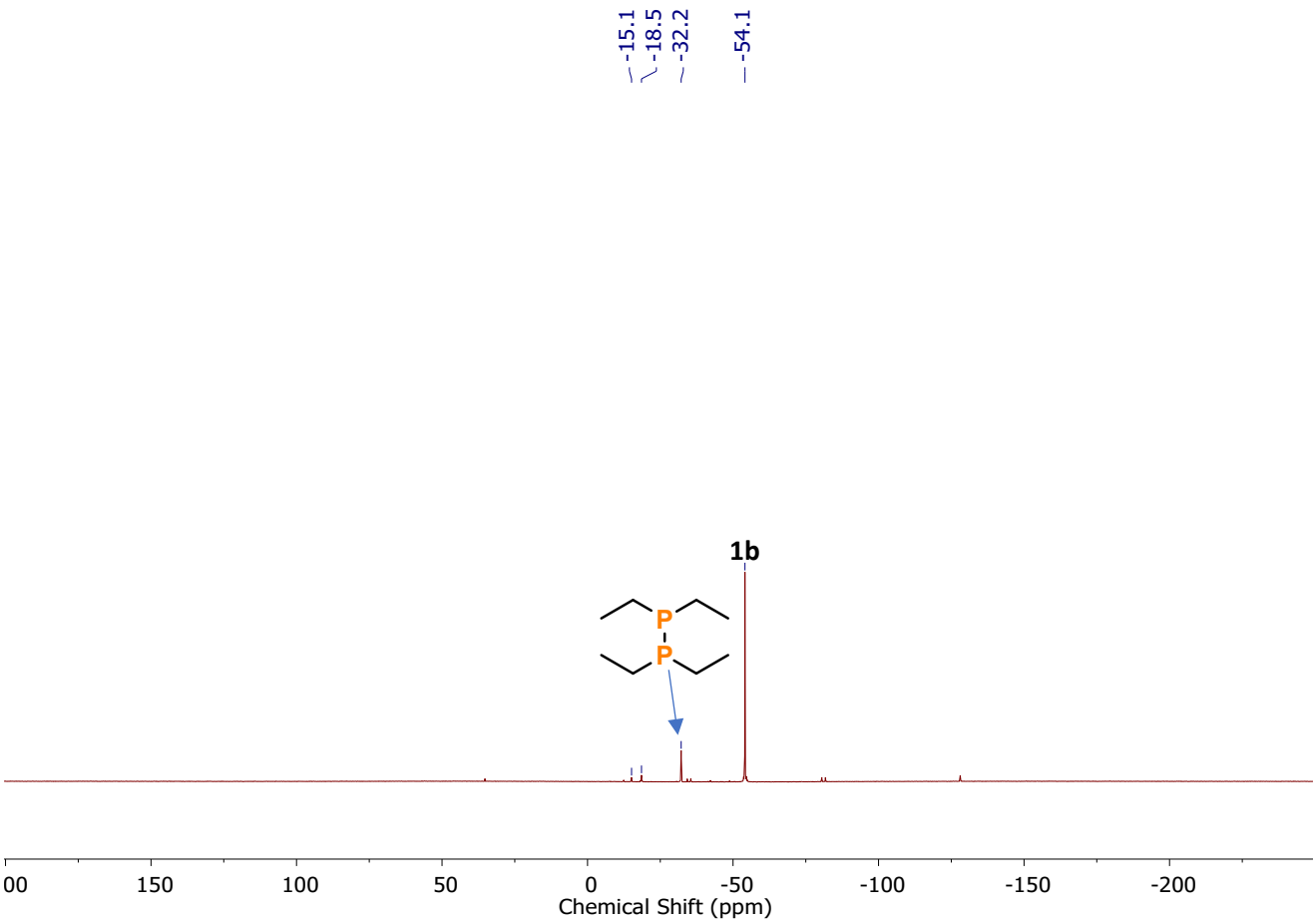

Figure S 3: $^{31}P\{^{1}H\}$ NMR spectrum of entry 4.

Control Reactions Using Freshly Distilled THF

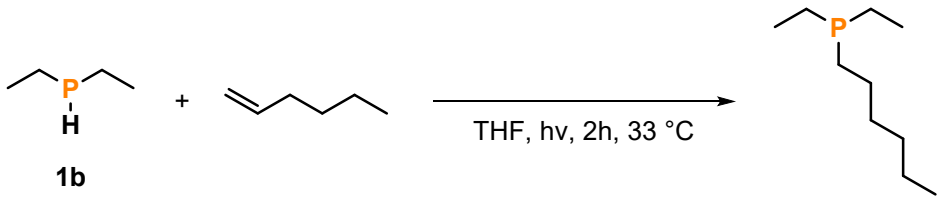

Quartz NMR tube or quartz tube – The two reactions were successful.

THF was dried and glass distilled from sodium/benzophenone. The reaction was carried out using the protocol outlined in a quartz tube and product formed, as identified from *in situ* $^{31}P\{^{1}H\}$ NMR spectra.

Testing THF for Peroxides

Distilled THF (0.9 mL) was transferred to a vial and a Bartovation peroxide test strip was dipped into the solvent for 1 second. Excess liquid was shaken off and after 10 seconds, the strip was compared against a colour chart. The test showed that qualitatively there was 0 ppm level of peroxide.

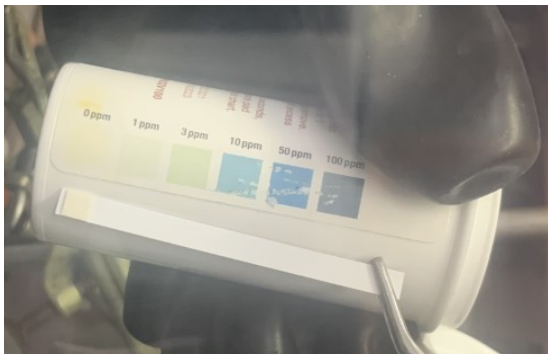

Reaction with UV Solution Filters

An aqueous solution of 1.77 M of $NiSO_4 \cdot H_2O$ and 0.29 M of $CoSO_4 \cdot H_2O$ was charged to a quartz sleeve (outer diameter = 30 mm). To a quartz tube (outer diameter = 12 mm), a solution of 1.16 x 10^{-4} M of 1,4 diphenyl butadiene in diethyl ether was charged. The quartz tube was then placed into the quartz sleeve. **3** (0.05 g, 0.2714 mmol, 1 equiv.), **1b (**0.04 g, 47 µL, 0.4072 mmol, 1.5 equiv.) and THF (0.9 mL) were charged into a quartz NMR tube. The NMR tube was placed into the quartz tube and the solutions were irradiated with UV light for 2 h. A thermometer was placed next to the UV setup to measure the temperature emitting from the lamp. The UV solution filters allowed percent transmission of 15% in the range of 245-270 nm (λ_{max} = 256 nm).[1,2] The reaction proceeded successfully.

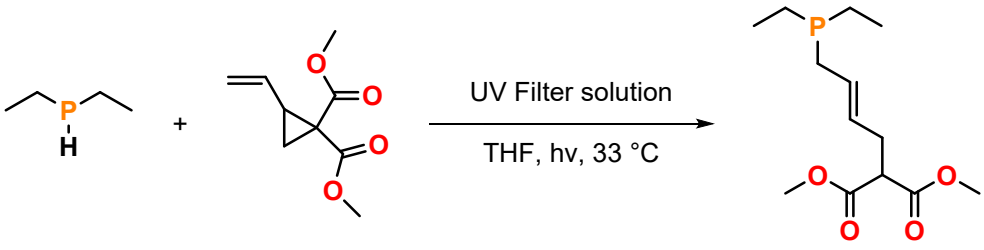

1b **3** **4b**

Ni: Light between 230 nm – 330 nm, 500 nm (peak) & 900 nm (peak) transmit through solution

Co: Light between 230nm – 250 nm filters through, solution absorbs at the IR and visible light regions

Butadiene: Light with a wavelength of 255 nm filters through solution. Absorbs light within 290 nm – 350 nm.

Ni/Co: Light within 240 nm – 320 nm is filtered. Also light at 500 nm and 900 nm transmits through the solution in small amounts. Absorbs light from 200 nm – 320 nm, and 320 nm – 1000 nm.

H_2O: Absorbs light with a wavelength of 900 nm

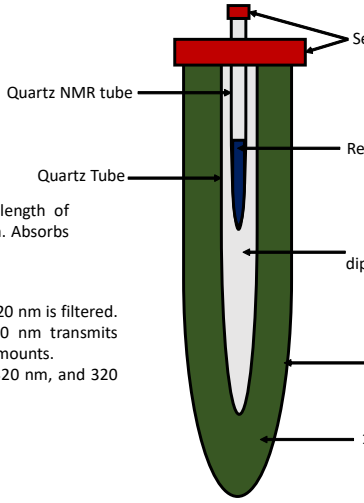

Ni/Co/butadiene: Filters through UV light within the range of 245-270 nm with a 15% transmission. λ_{max} = 256 nm. Also allows light to transmit at 570 nm with a 1.5% (filter defect)

Figure S 4: UV solution filter reaction setup next to a mercury lamp/immersion well. Bottom figure describes the above picture. Note: The experimental setup for photolysis precludes our ability to heat or cool the reaction. A thermometer was placed within the enclosure of the UV-light box as a proxy for the reaction temperature.

UV-Vis Spectrum of **1b**, **3** & Mixture of **1b** + **3**

All samples had a concentration of 8.14×10^{-4} M in THF.

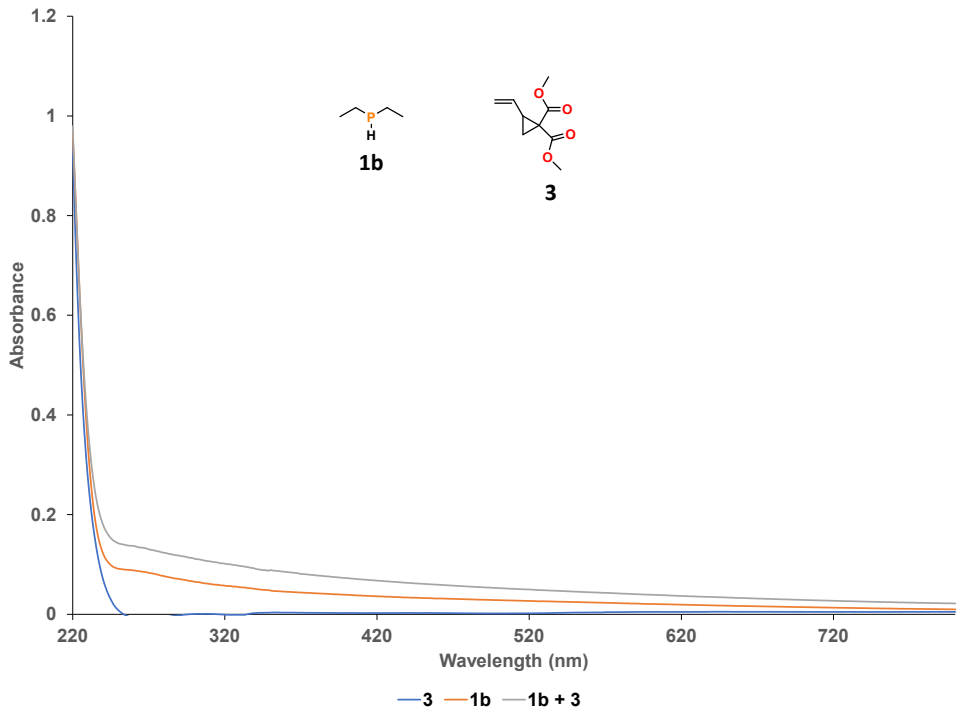

Figure S 5: UV-Vis absorbance spectrum of 3, 1b, and 1b + 3.

Spectra and High-Resolution Mass Spectrometry of Control Reactions

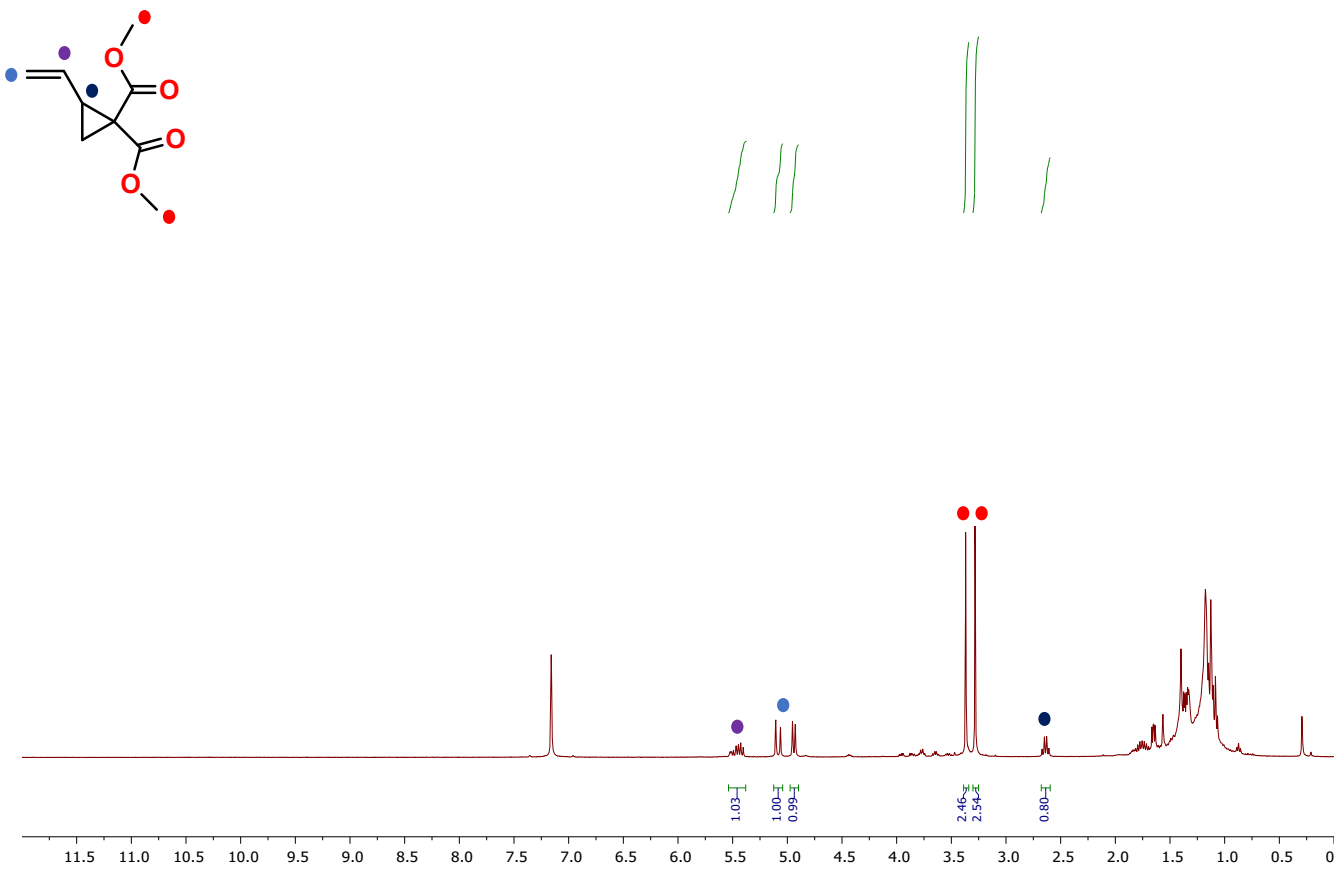

Figure S 6: Crude ^{1}H NMR spectrum of radical trapping experiment using 1 equiv. of TEMPO (entry 6) recorded in $CDCl_3$.

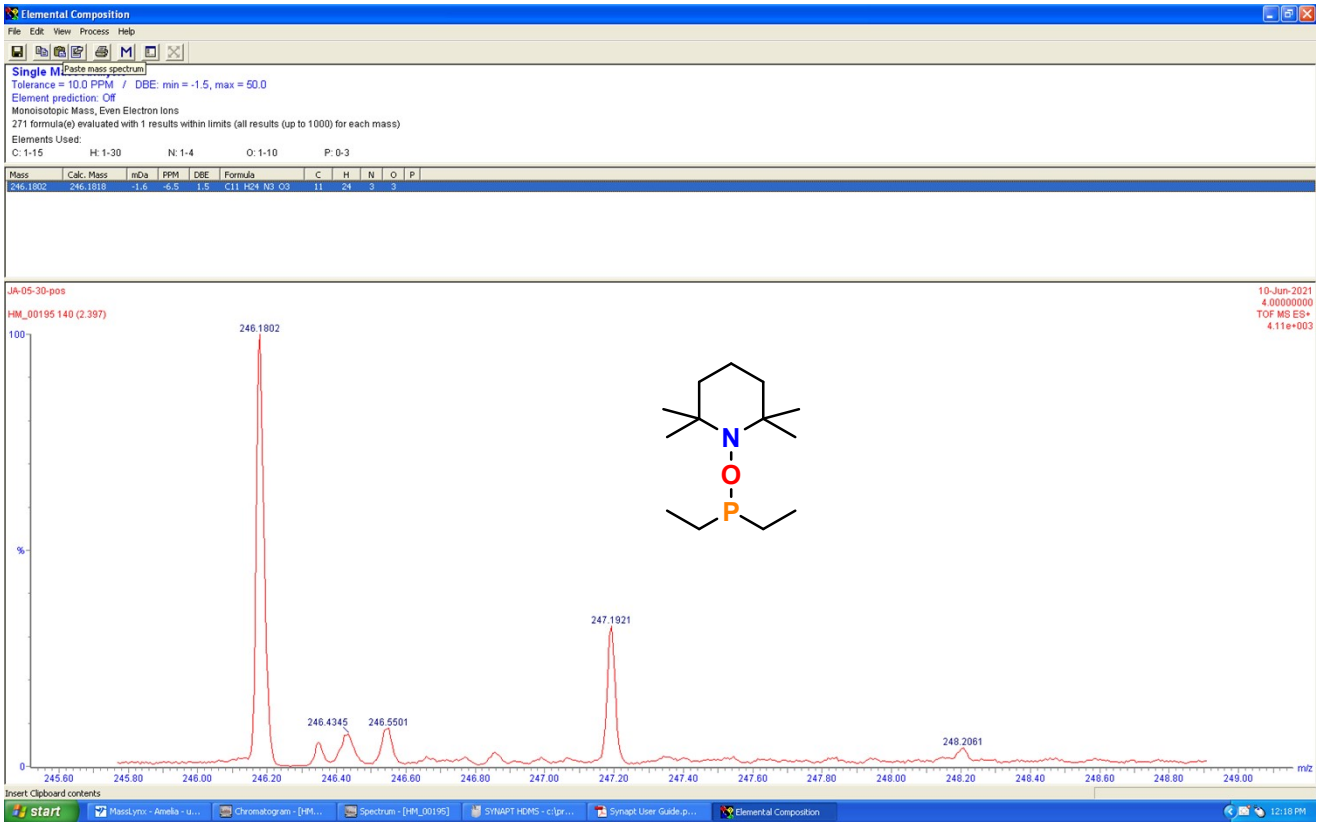

Figure S 7: HRMS of radical trapping experiment using 1 equiv. of TEMPO (entry 6).

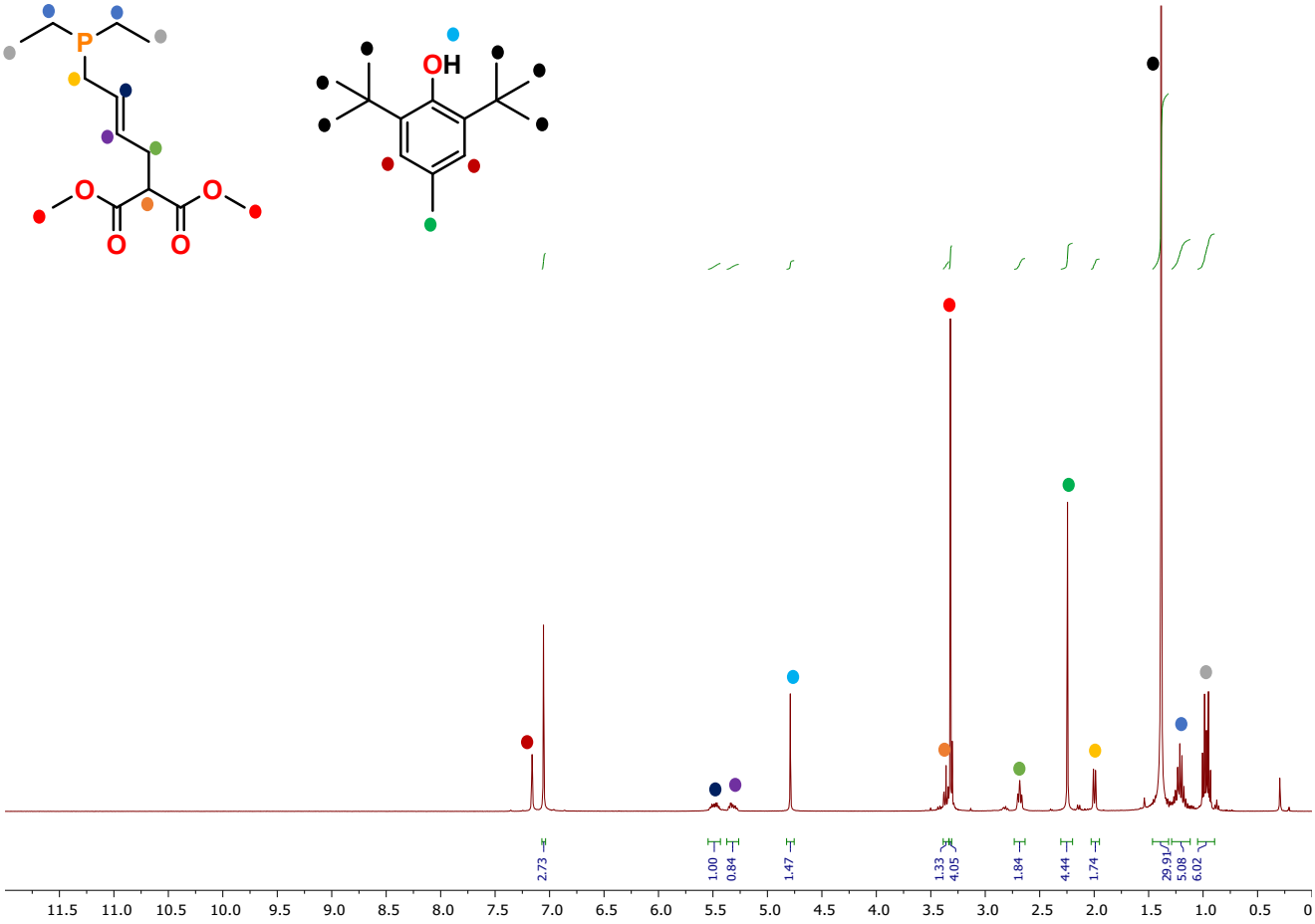

Figure S 8: Crude ^{1}H NMR spectrum of radical trapping experiment using 1 equiv. of BHT (entry 7) recorded in $CDCl_3$.

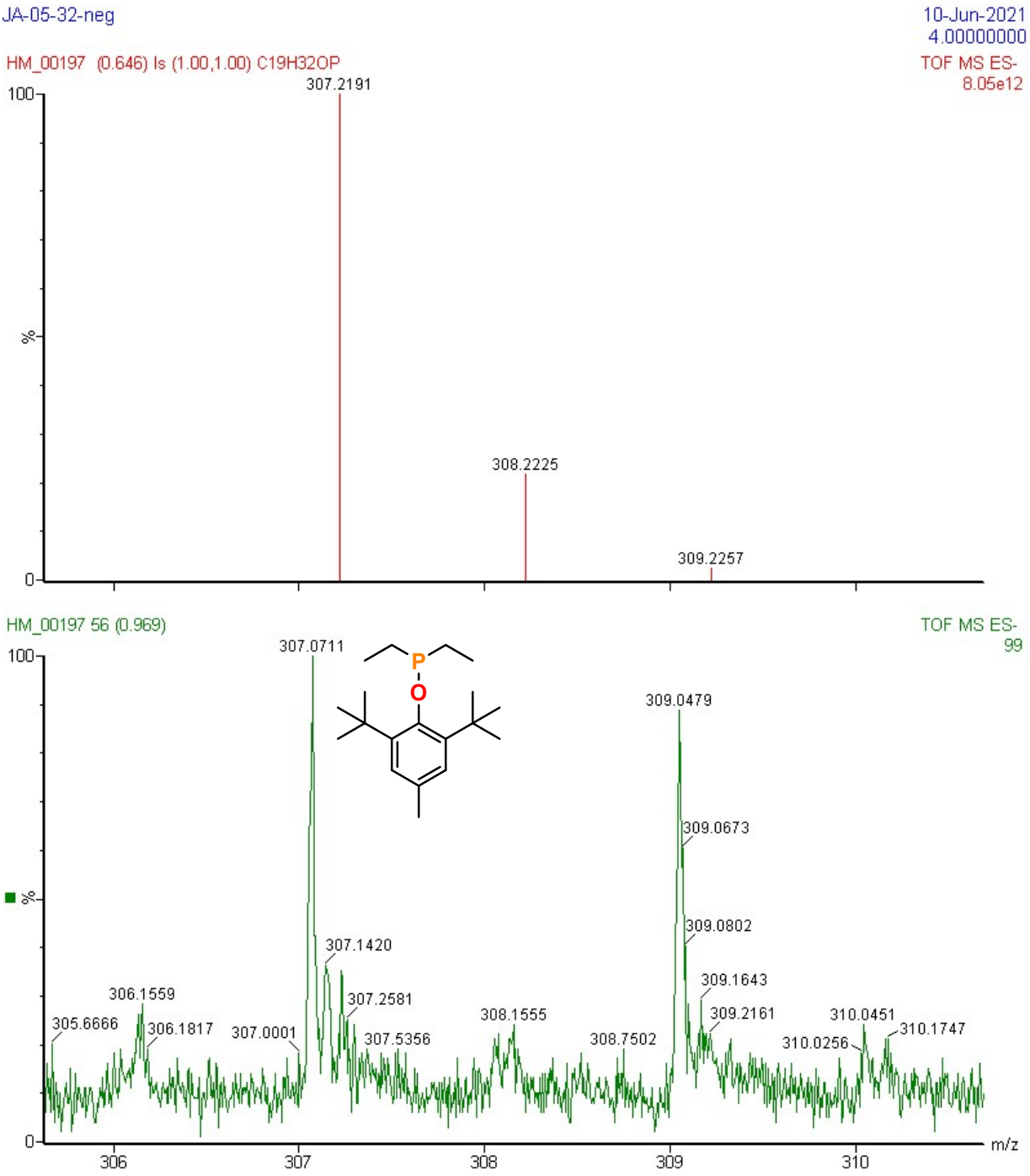

Figure S 9: HRMS of radical trapping experiment using 1 equiv. of BHT (entry 7).

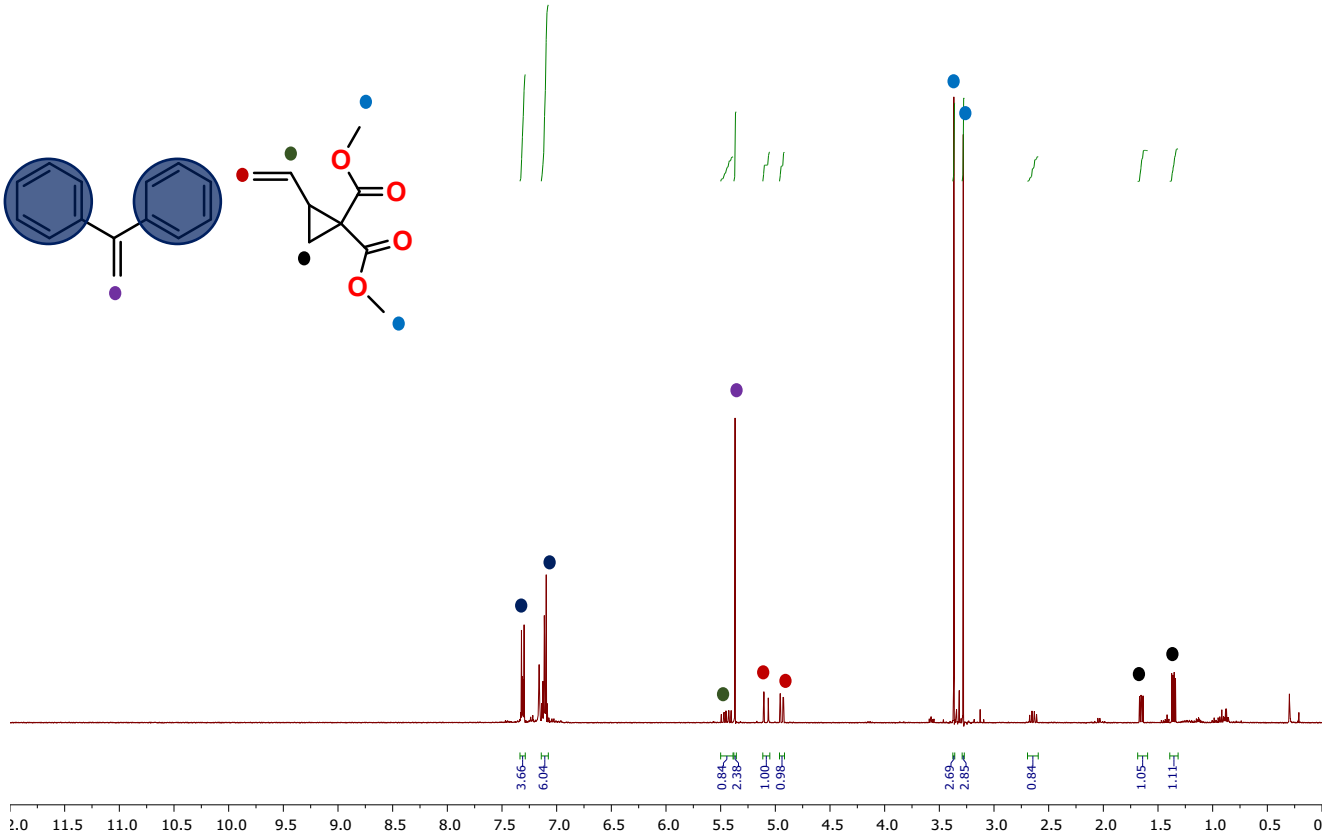

Figure S 10: Crude ^{1}H NMR spectrum of radical trapping experiment using 1 equiv. of DPE (entry 8) recorded in $CDCl_3$.

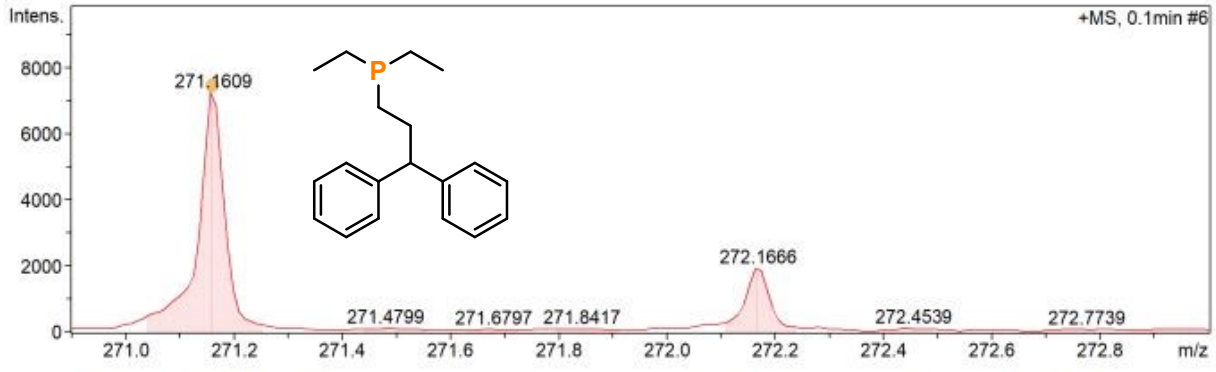

Meas. m/z	#	Ion Formula	m/z	err [ppm]	mSigma	# mSigma	Score	rdb	e¯ Conf	N-Rule
271.1609	1	C18H24P	271.1610	0.4	119.3	1	100.00	7.5	even	ok
275.1415	1	C13H24O4P	275.1407	-3.2	24.1	1	100.00	2.5	even	ok

Figure S 11: HRMS of radical trapping experiment using 1 equiv. of DPE (entry 8).

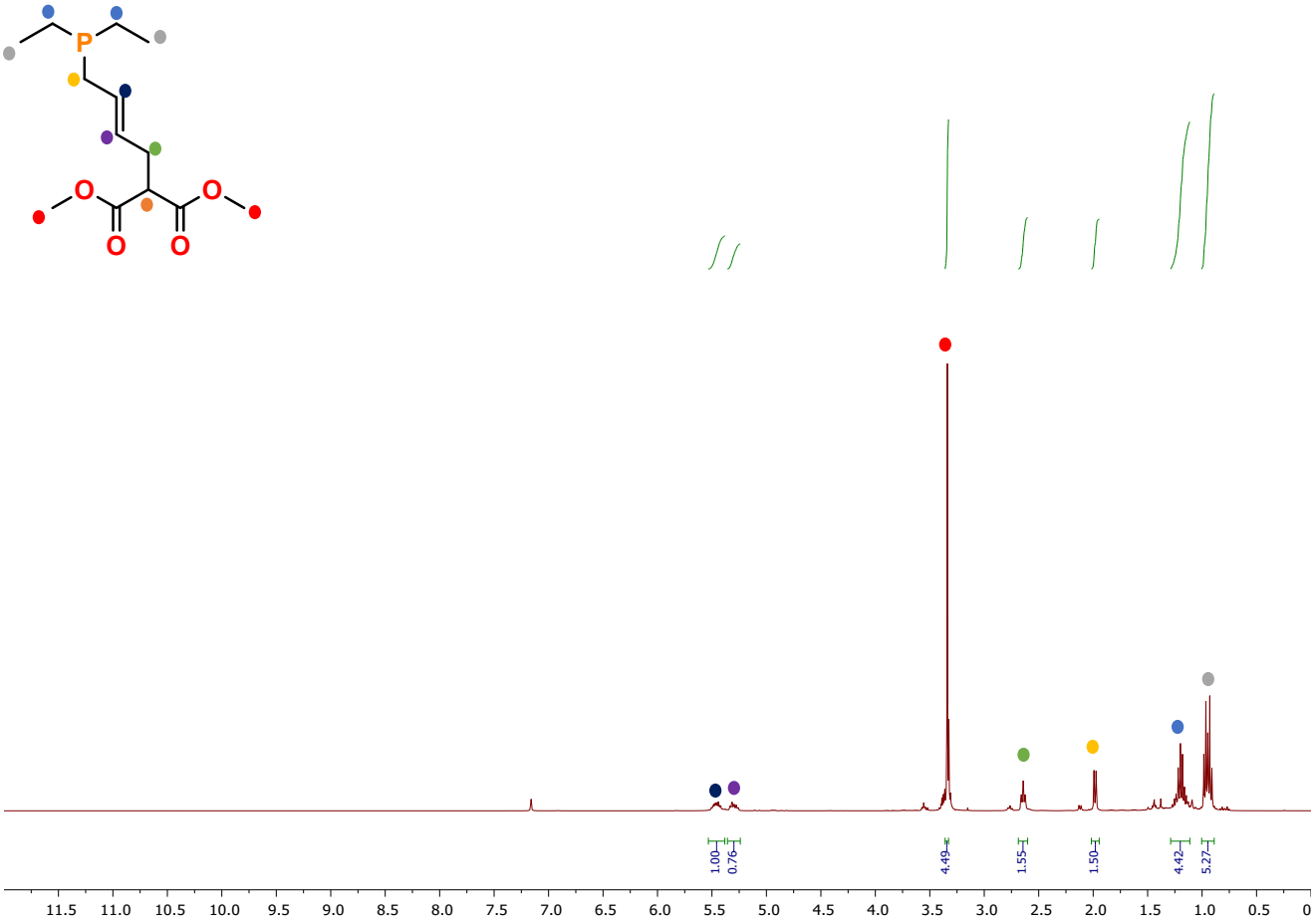

Figure S 12: Crude ^{1}H NMR spectrum of radical trapping experiment using 10 mol% of TEMPO (entry 9) recorded in $CDCl_3$.

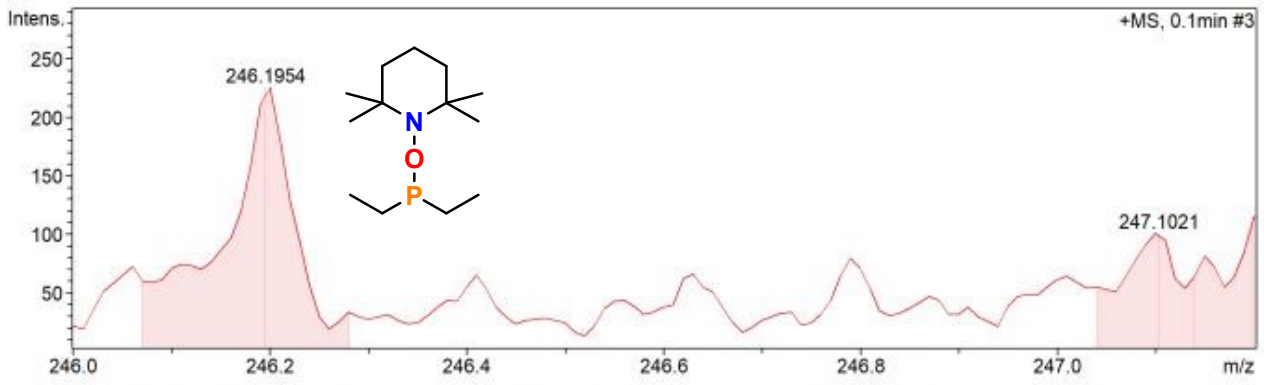

Meas. m/z	#	Ion Formula	m/z	err [ppm]	mSigma	# mSigma	Score	rdb	e¯ Conf	N-Rule
246.1954	1	C13H29NOP	246.1981	11.1	394.5	1	100.00	0.5	even	ok
275.1407	1	C13H24O4P	275.1407	-0.2	36.3	1	100.00	2.5	even	ok

Figure S 13: HRMS of radical trapping experiment using 10 mol% of TEMPO (entry 9).

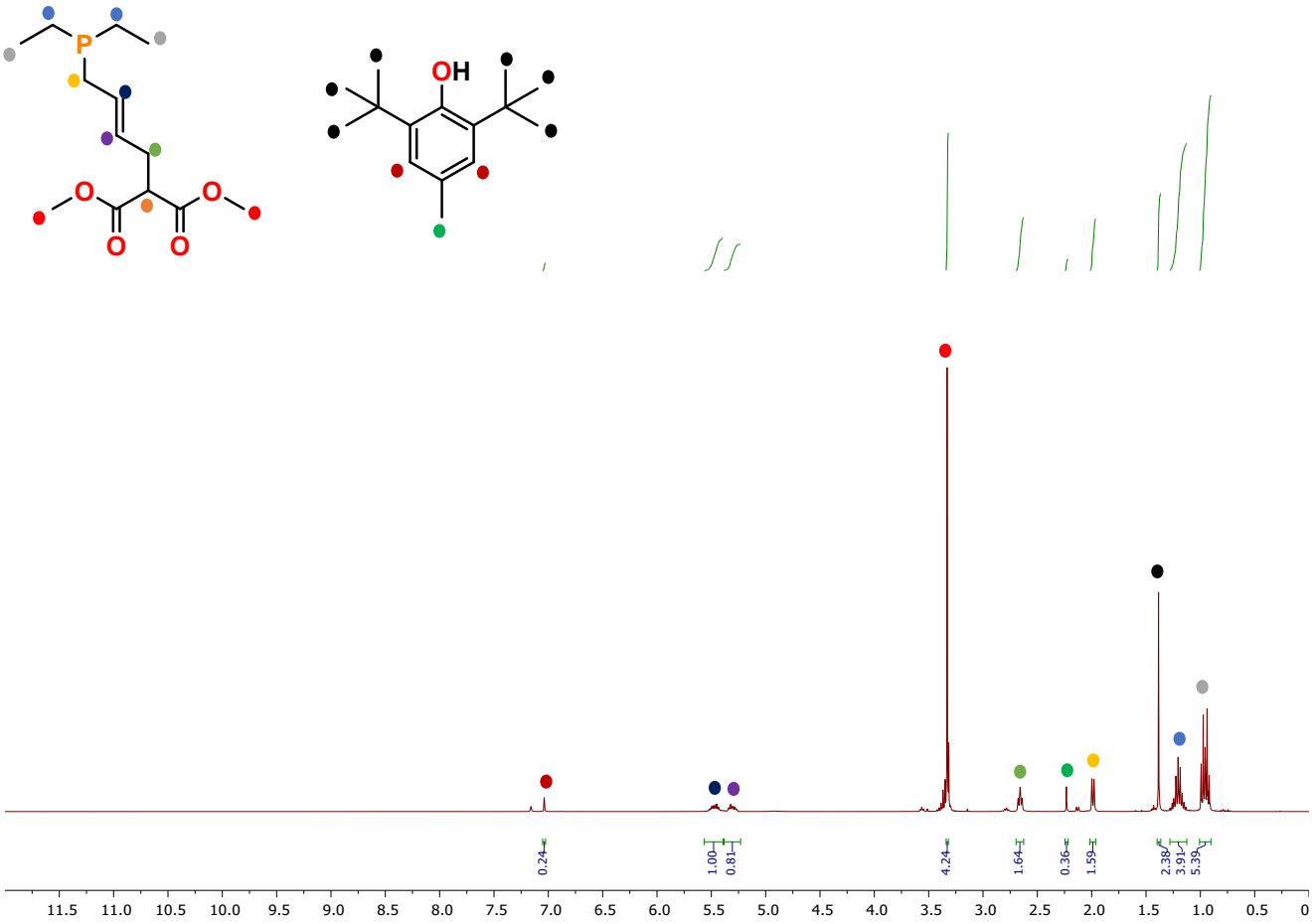

Figure S 14: Crude ^{1}H NMR spectrum of radical trapping experiment using 10 mol% of BHT (entry 10) recorded in $CDCl_3$.

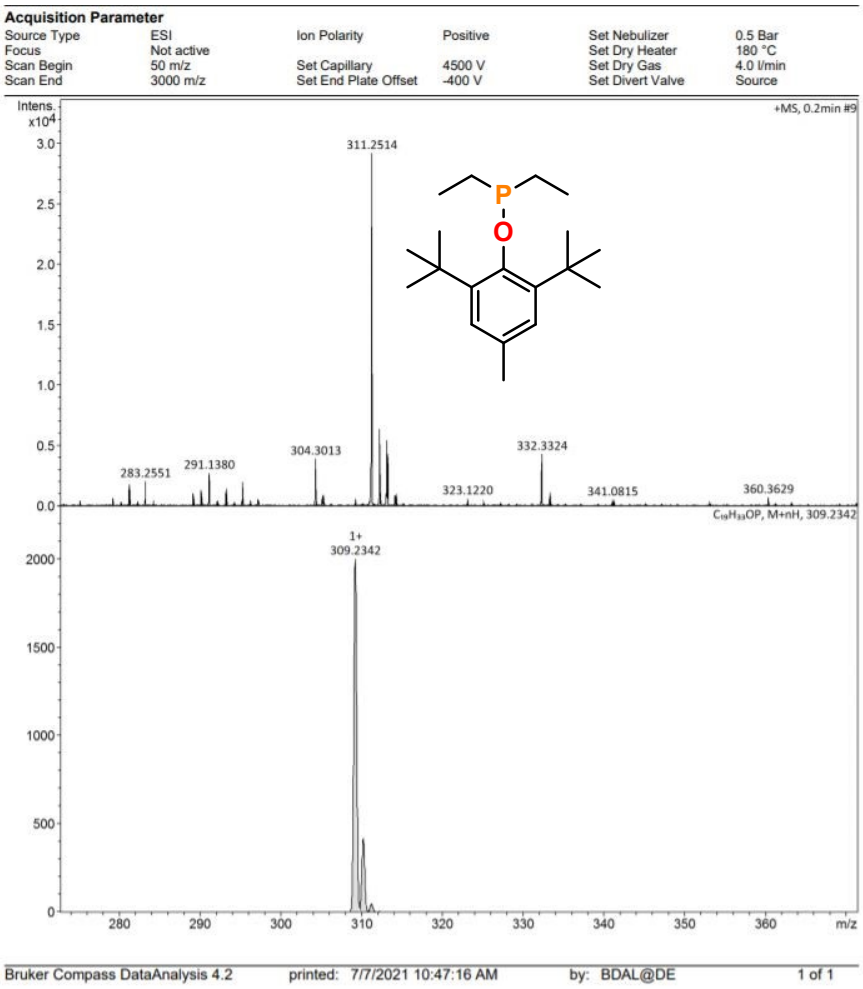

Figure S 15: HRMS of radical trapping experiment using 10 mol% of BHT (entry 10).

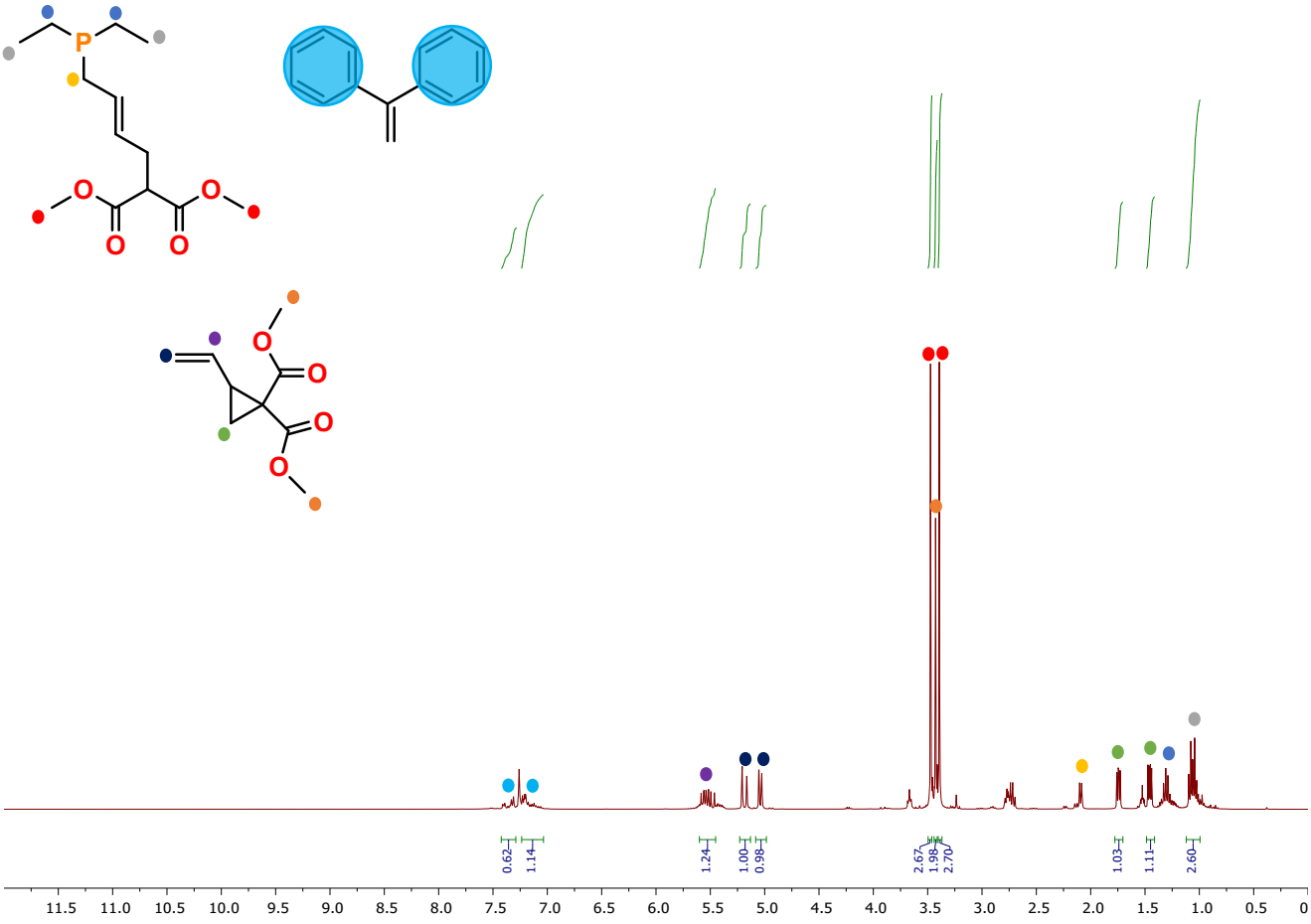

Figure S 16: Crude ^{1}H NMR spectrum of radical trapping experiment using 10 mol% of DPE (entry 11) recorded in $CDCl_3$.

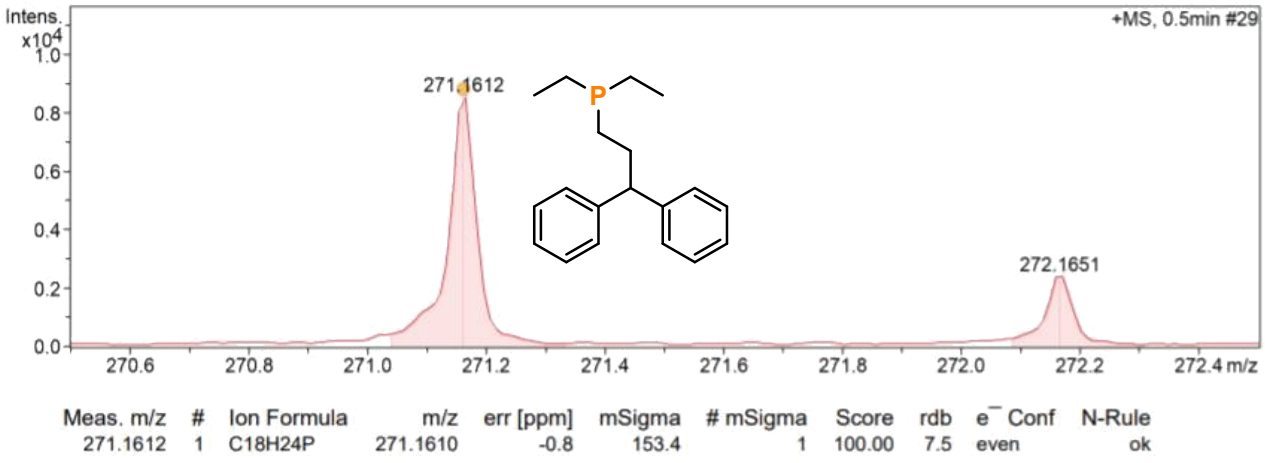

Figure S 17: HRMS of radical trapping experiment using 10 mol% of DPE (entry 11).

NMR Characterization of Phosphines, Phosphine Sulfides and Phosphine Oxide

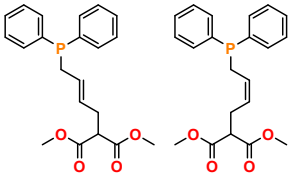

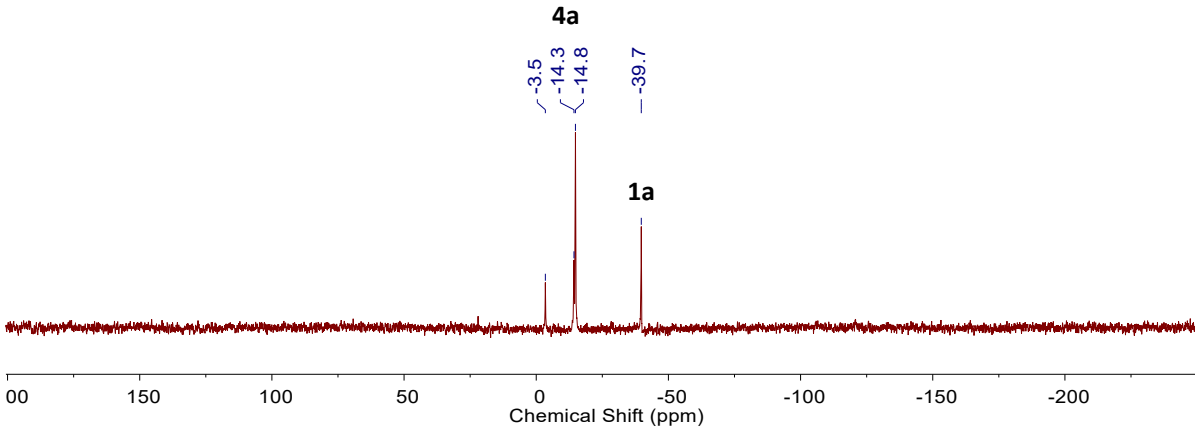

Figure S 18: $^{31}P\{^{1}H\}$ NMR spectrum of 4a recorded in $CDCl_3$.

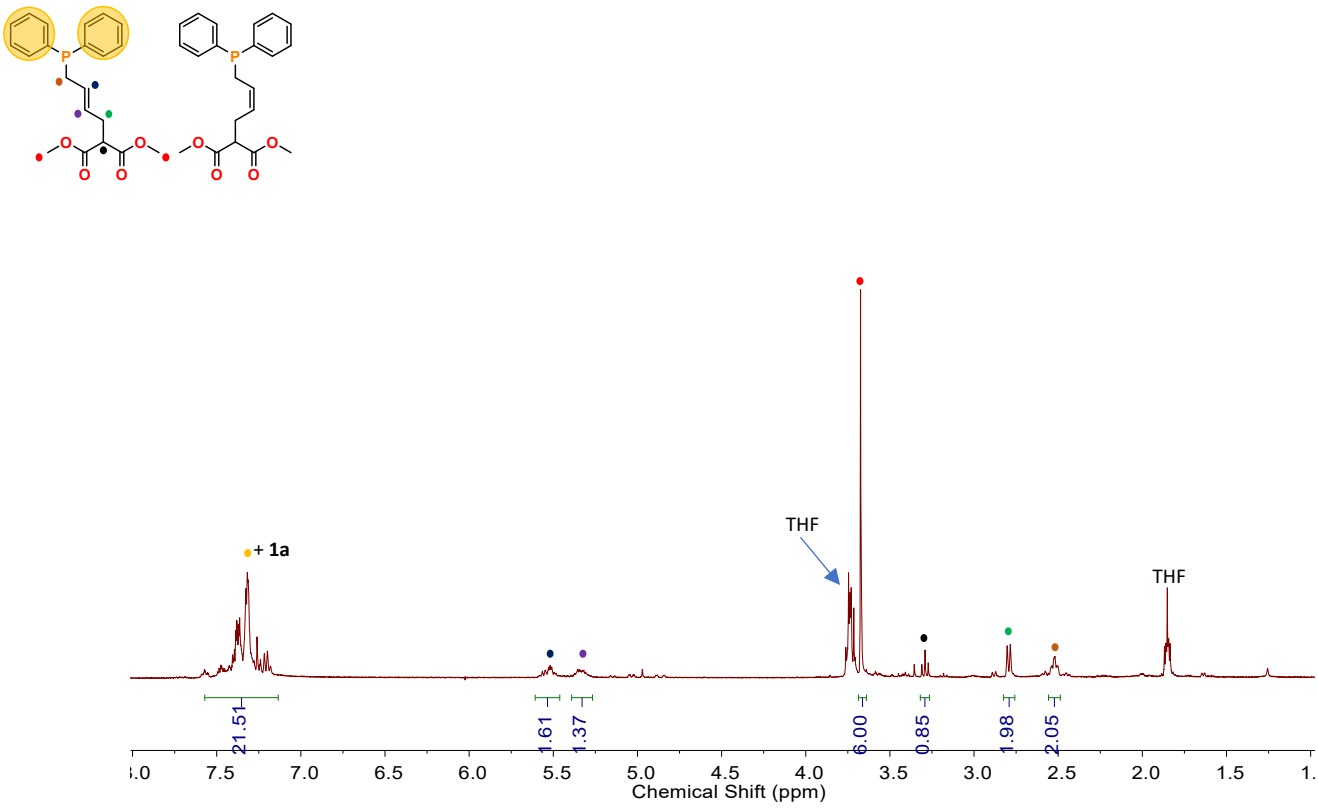

Figure S 19: ^{1}H NMR spectrum of isolated 4a recorded in $CDCl_3$.

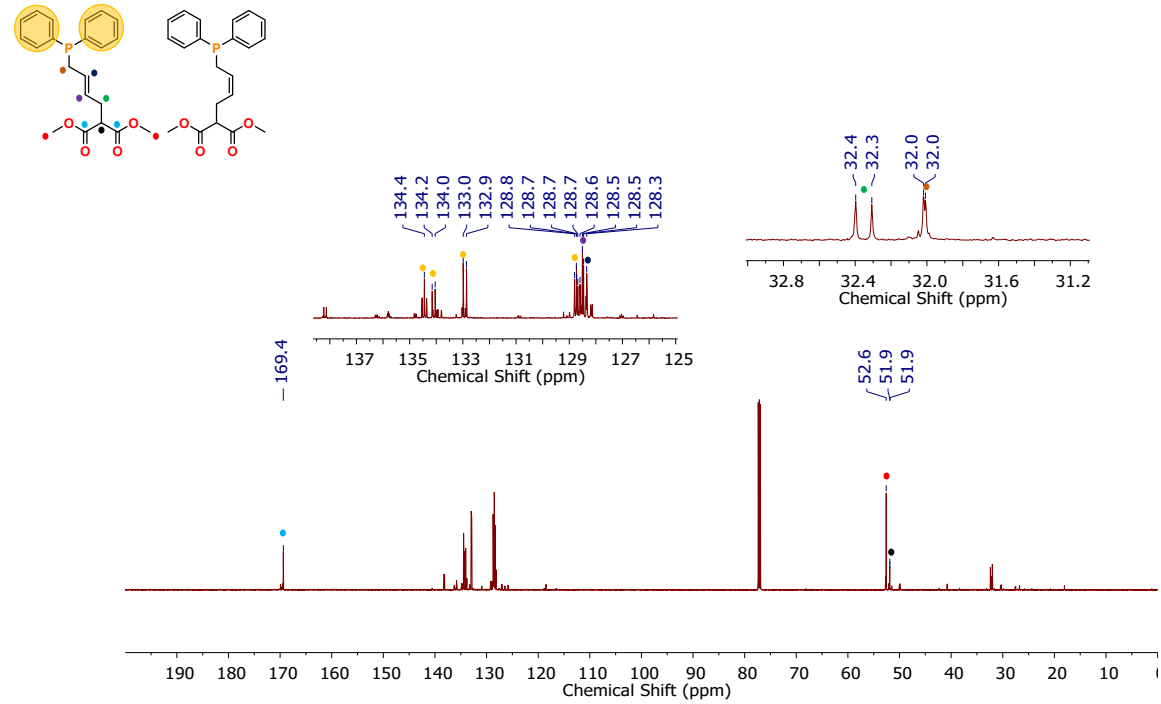

Figure S 20: $^{13}C\{^{1}H\}$ NMR spectrum of 4a recorded in $CDCl_3$.

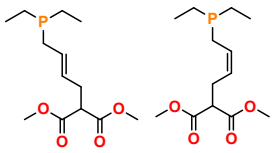

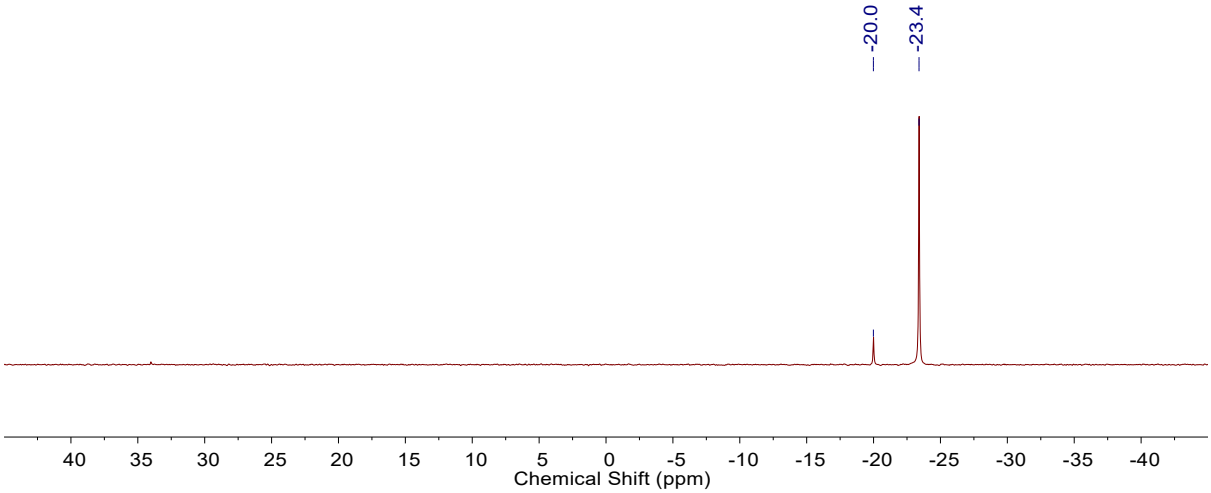

Figure S 21: $^{31}P\{^{1}H\}$ NMR spectrum of 4b recorded in C_6D_6.

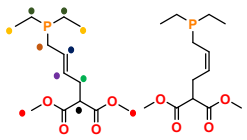

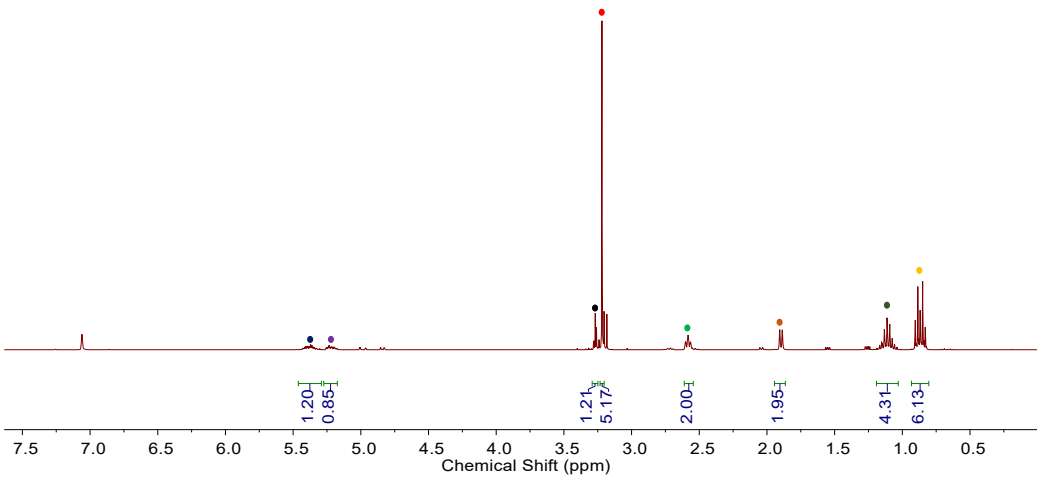

Figure S 22: ^{1}H NMR spectrum of 4b recorded in C_6D_6.

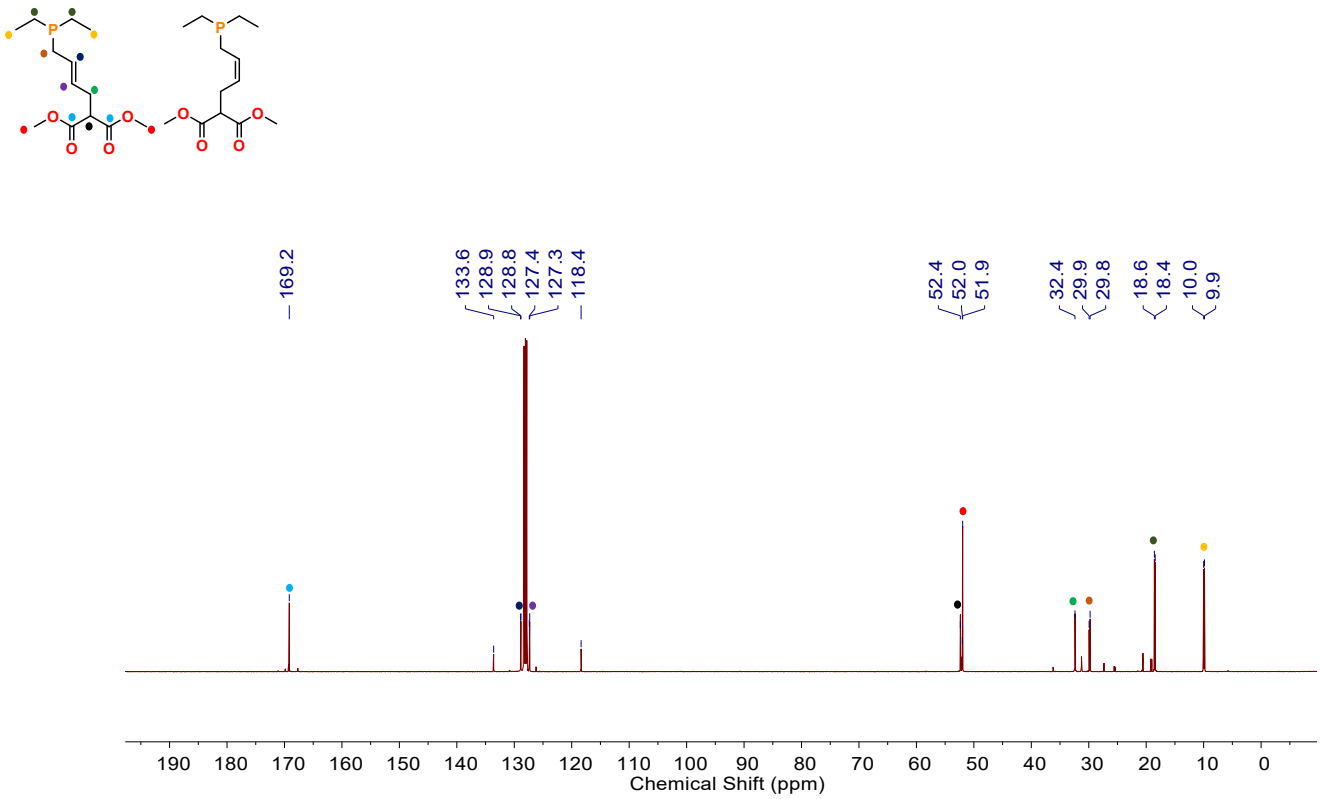

Figure S 23: $^{13}C\{^{1}H\}$ NMR spectrum of 4b recorded in C_6D_6.

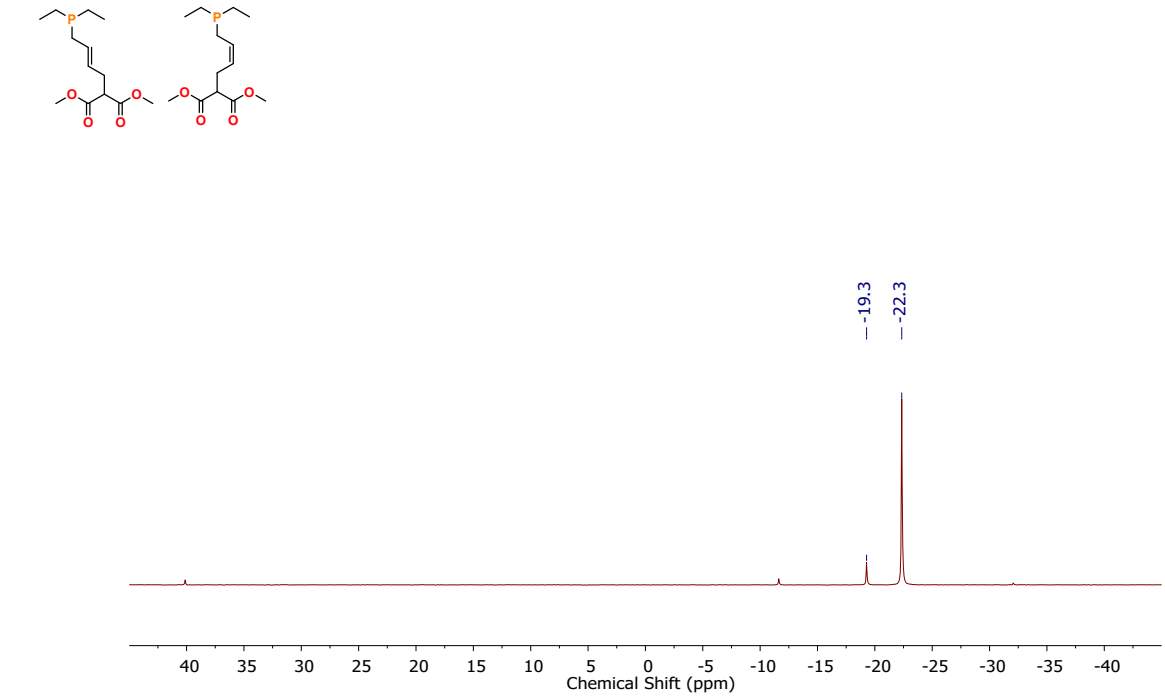

Figure S 24: $^{31}P\{^{1}H\}$ NMR spectrum of 4b (scaled up) recorded in $CDCl_3$.

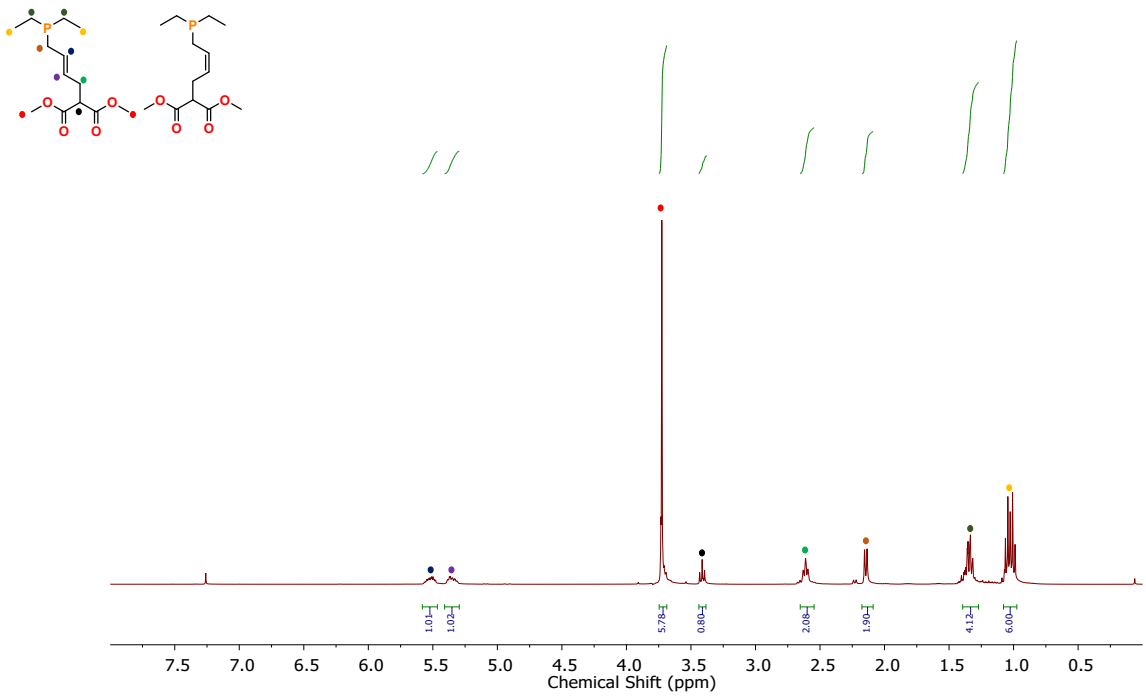

Figure S 25: ^{1}H NMR spectrum of 4b (scaled up) recorded in $CDCl_3$.

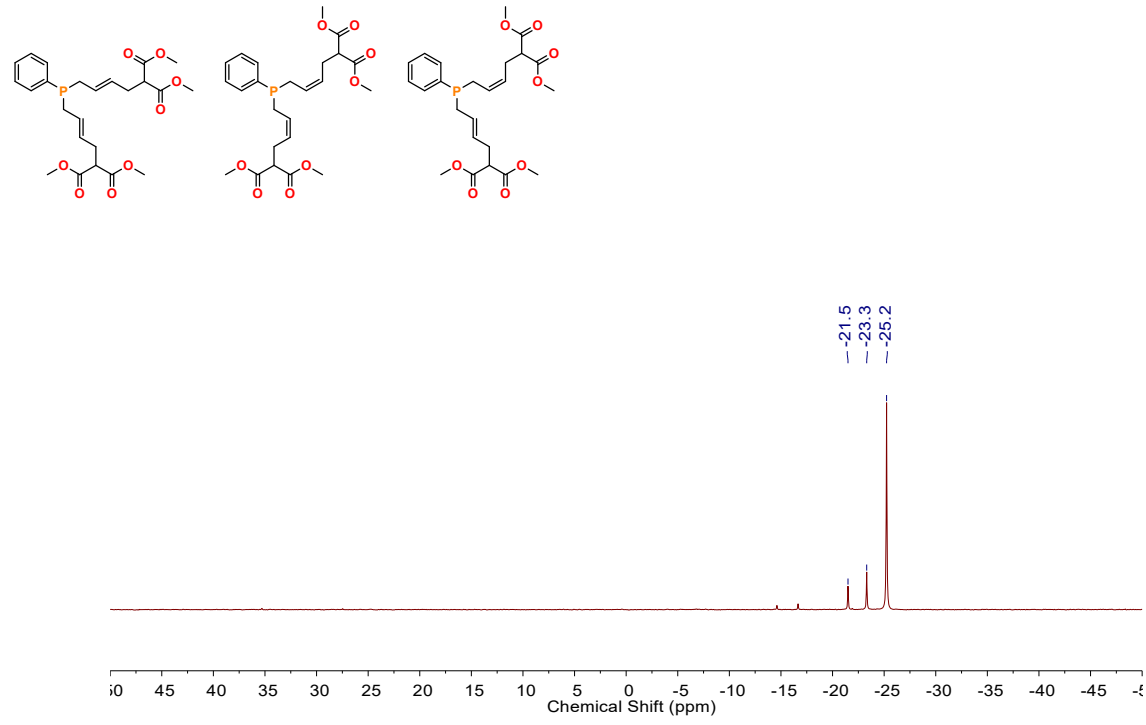

Figure S 26: $^{31}P\{^{1}H\}$ NMR spectrum of 5a recorded in $CDCl_3$.

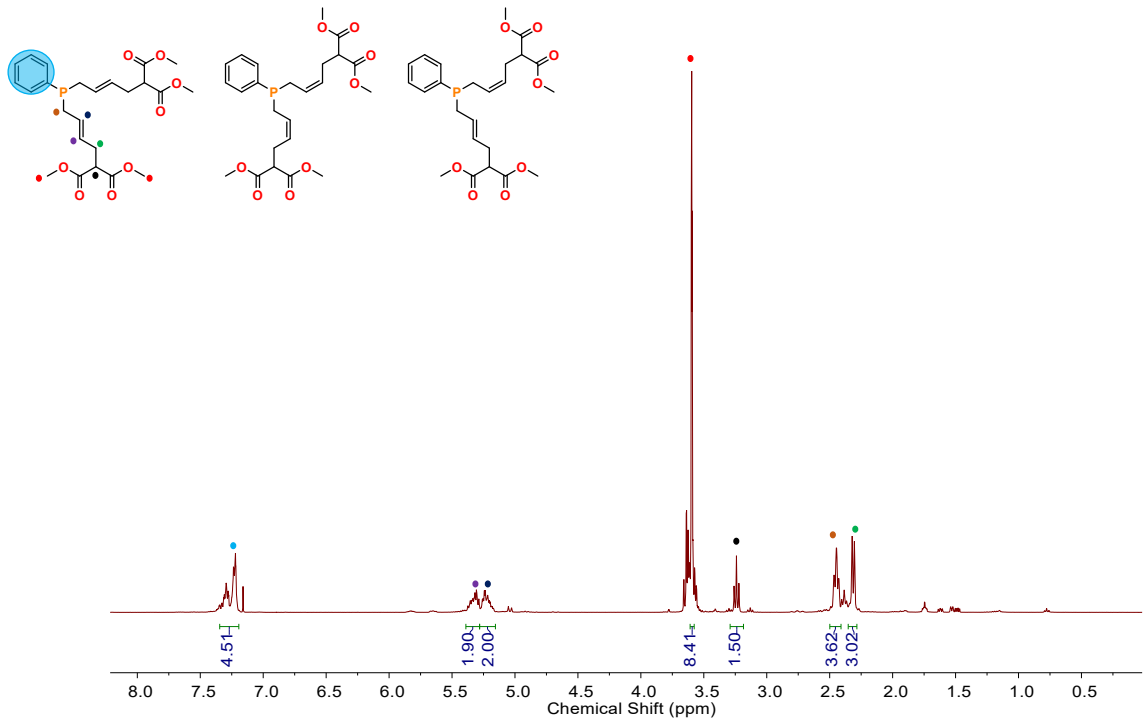

Figure S 27: ^{1}H NMR spectrum of 5a recorded in $CDCl_3$.

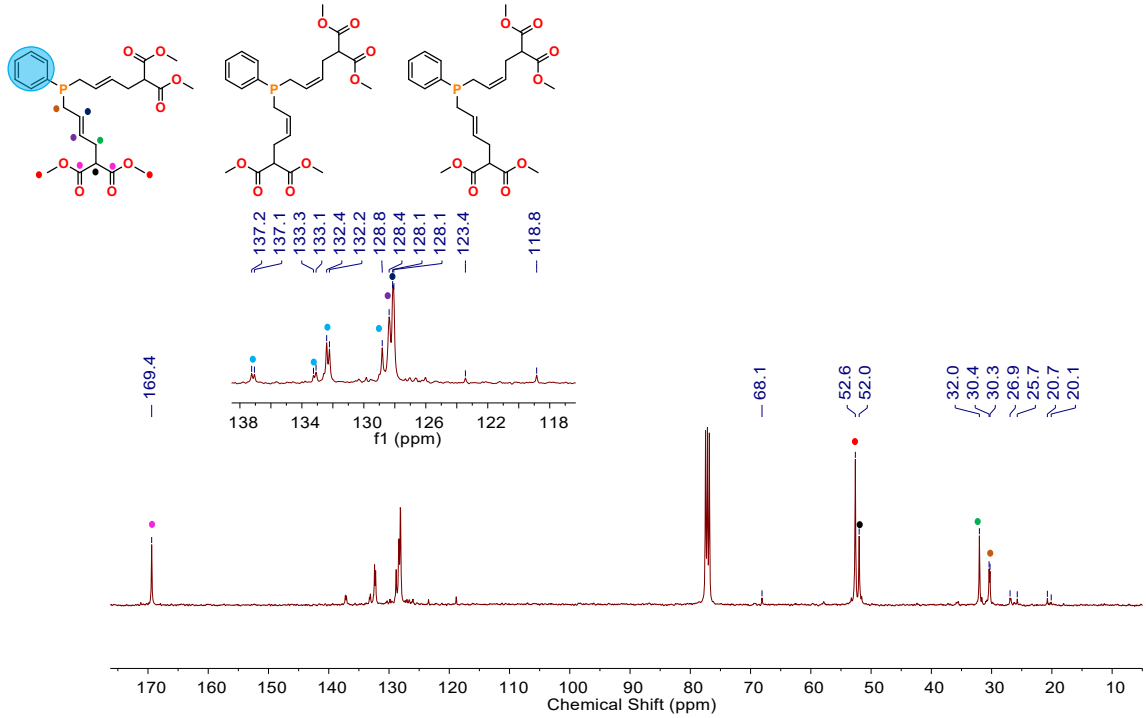

Figure S 28: $^{13}C\{^{1}H\}$ NMR spectrum of 5a recorded in $CDCl_3$.

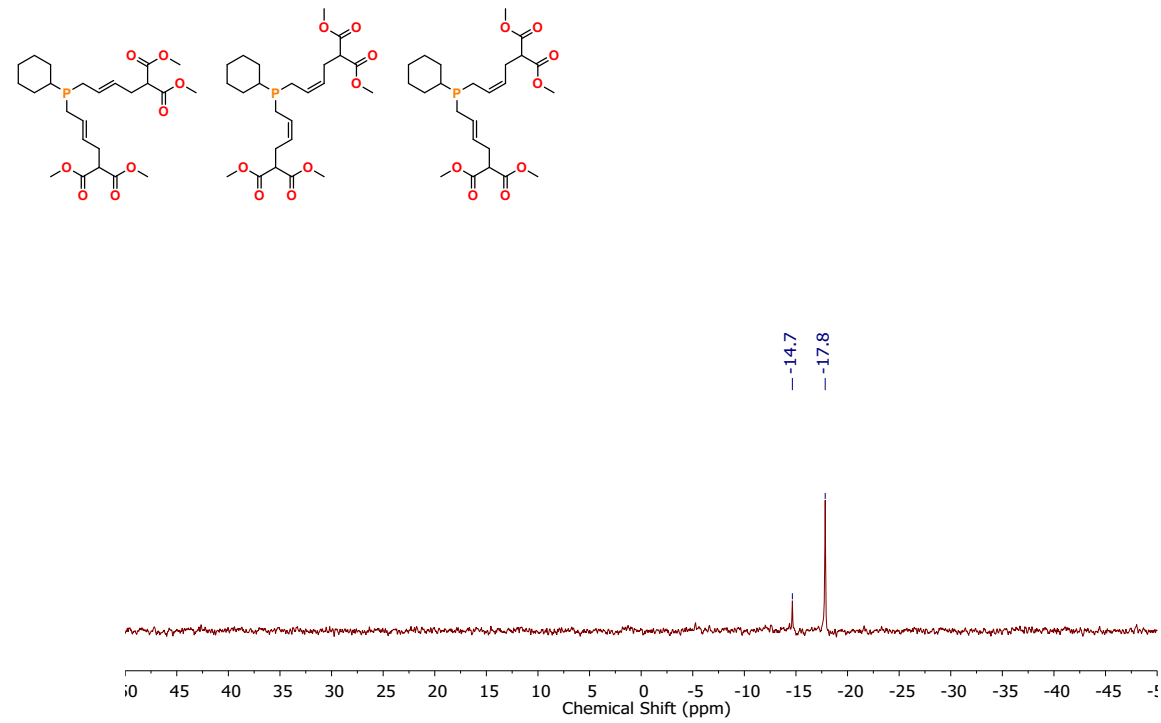

Figure S 29: $^{31}P\{^{1}H\}$ NMR spectrum of 5b recorded in $CDCl_3$.

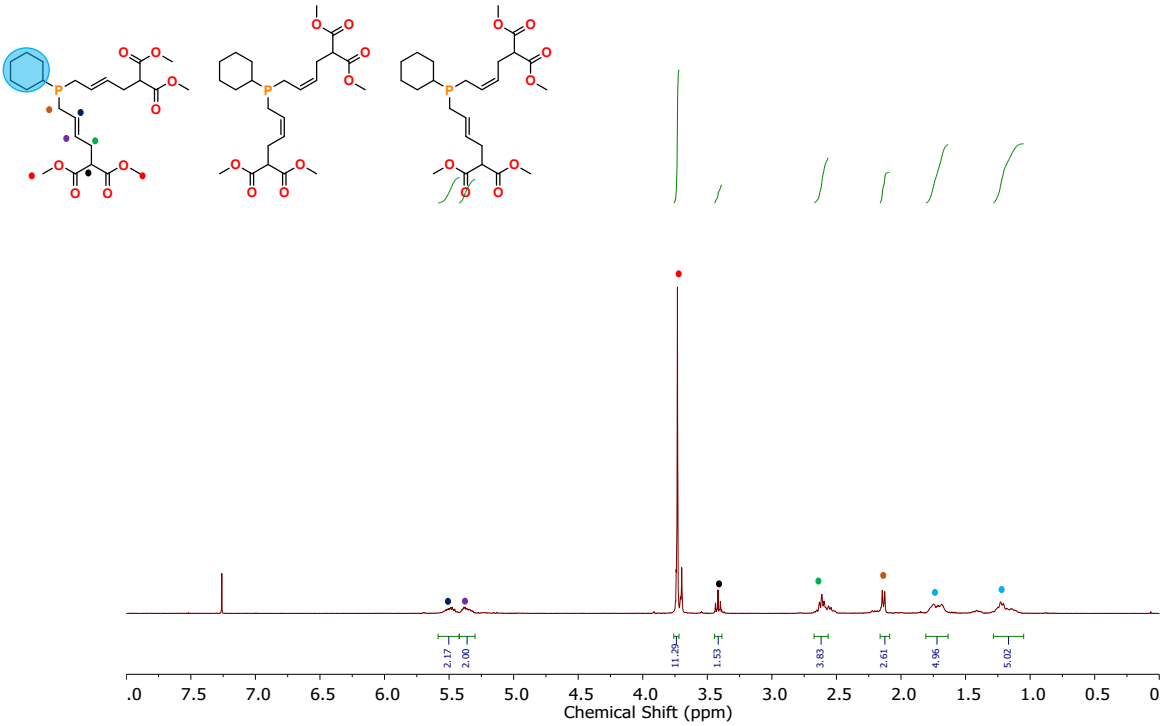

Figure S 30: ^{1}H NMR spectrum of 5b recorded in $CDCl_3$.

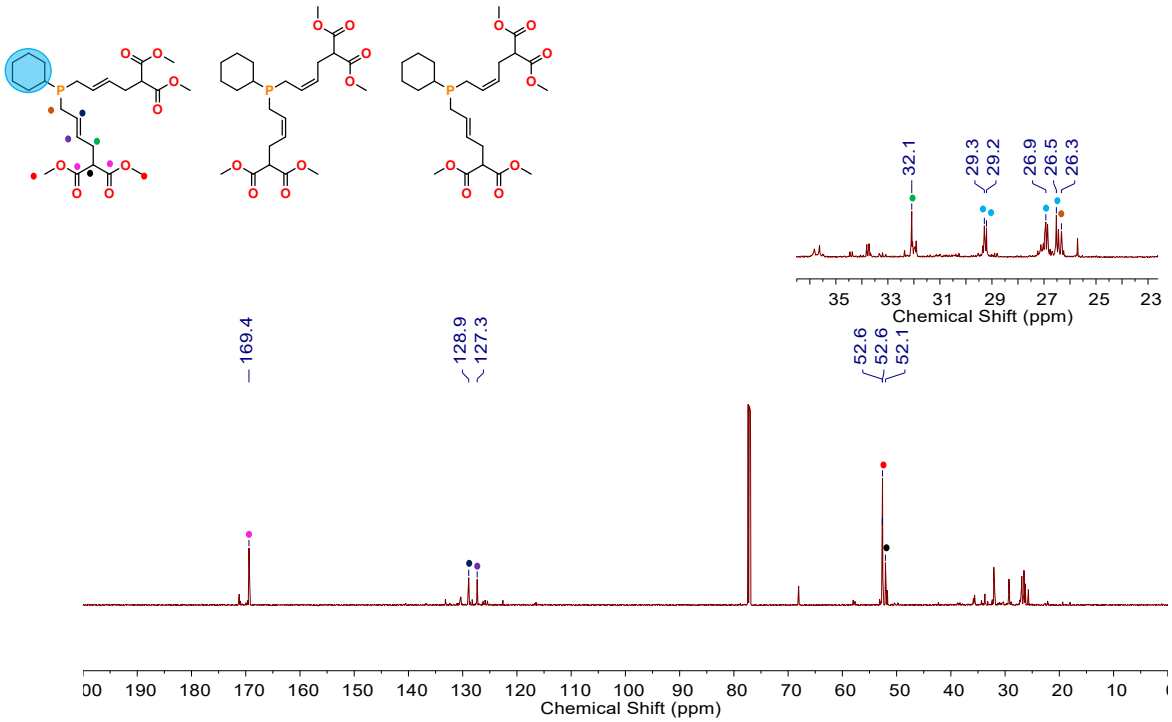

Figure S 31: $^{13}C\{^{1}H\}$ NMR spectrum of 5b recorded in $CDCl_3$.

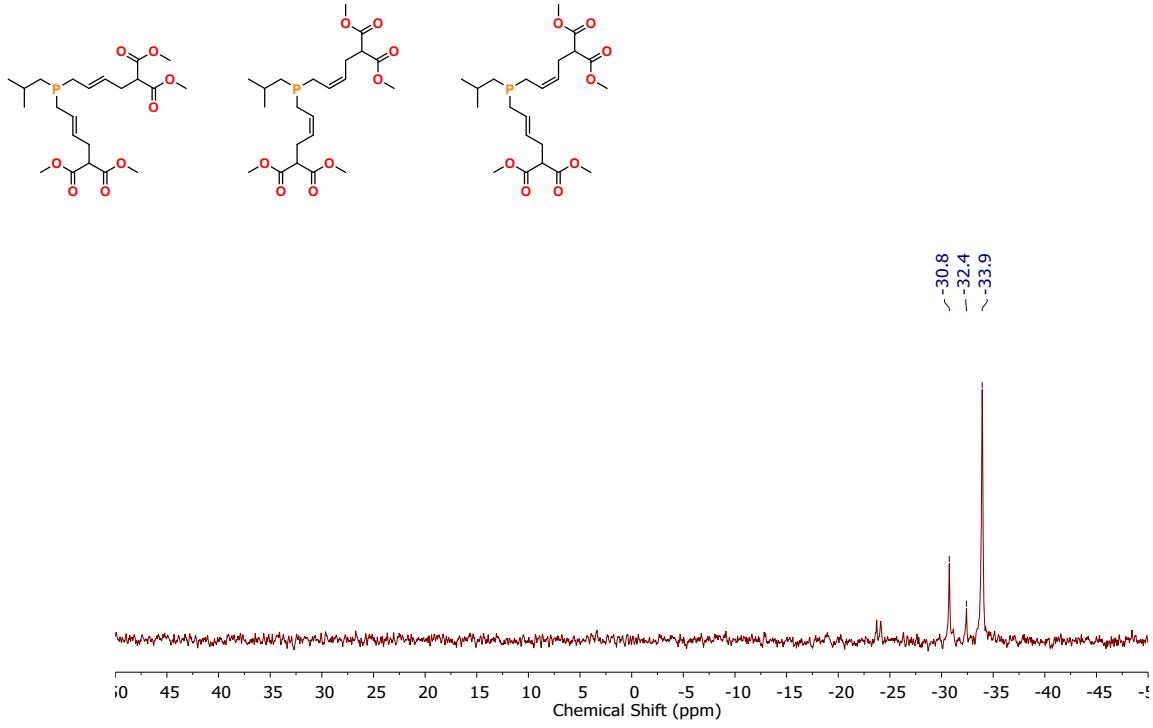

Figure S 32: $^{31}P\{^{1}H\}$ NMR spectrum of 5c recorded in C_6D_6.

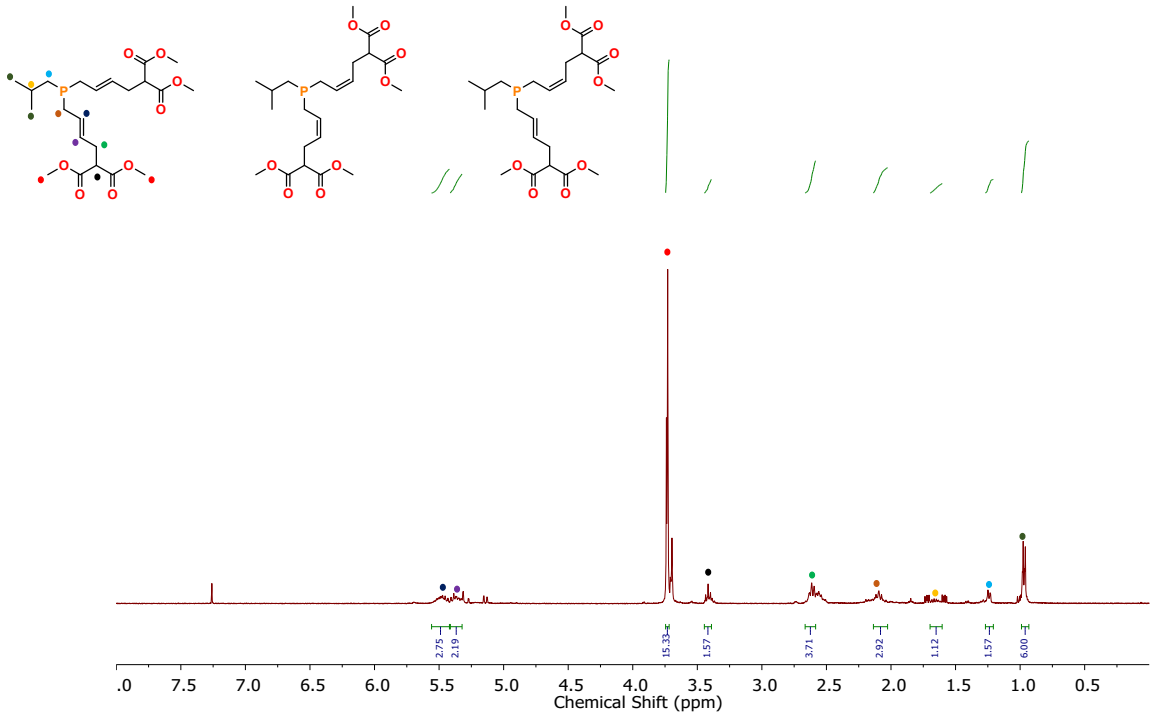

Figure S 33: ^{1}H NMR spectrum of 5c recorded in C_6D_6.

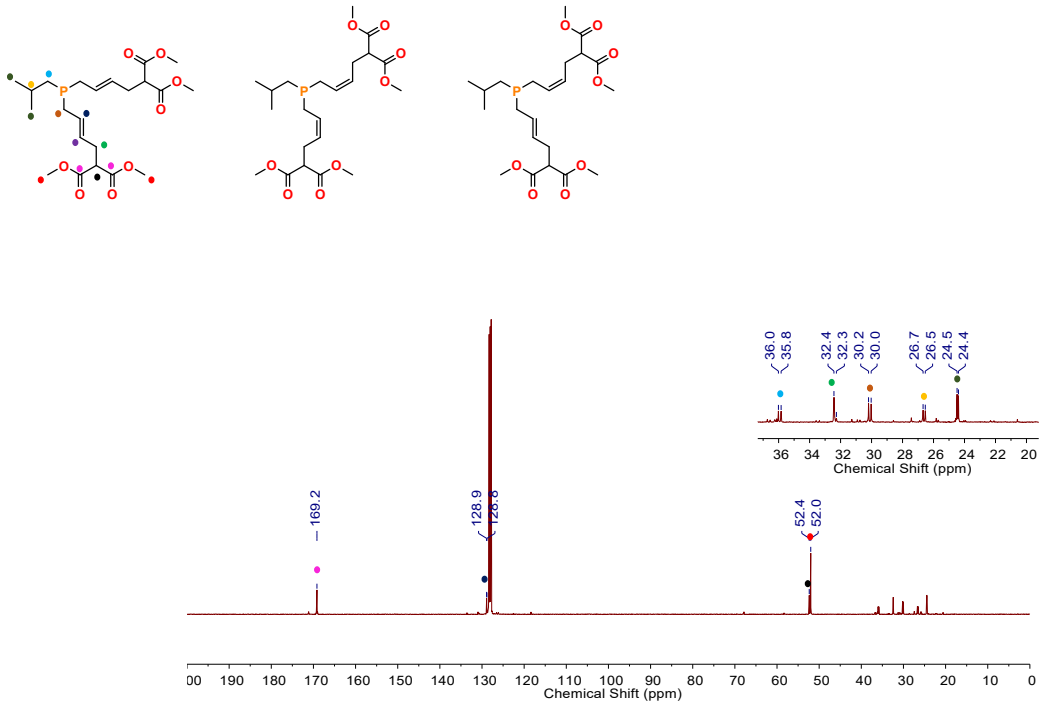

Figure S 34: ^{13}C{^{1}H} NMR spectrum of 5c recorded in C_6D_6.

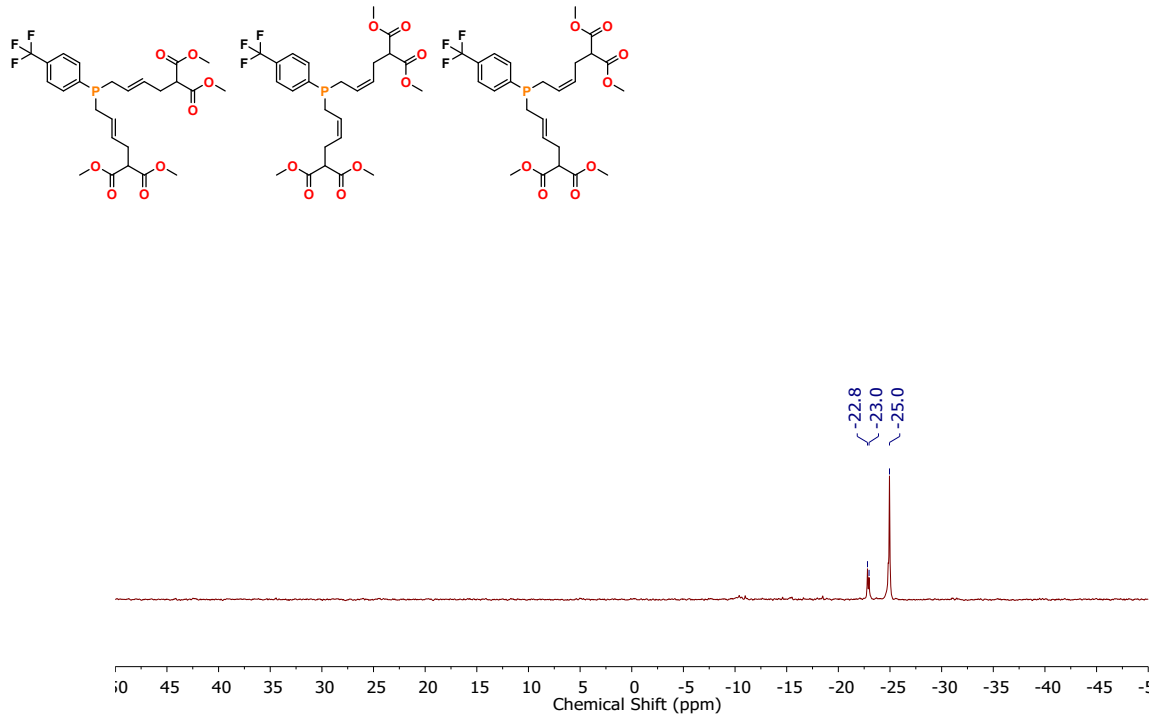

Figure S 35: $^{31}P\{^{1}H\}$ NMR spectrum of 5d recorded in $CDCl_3$.

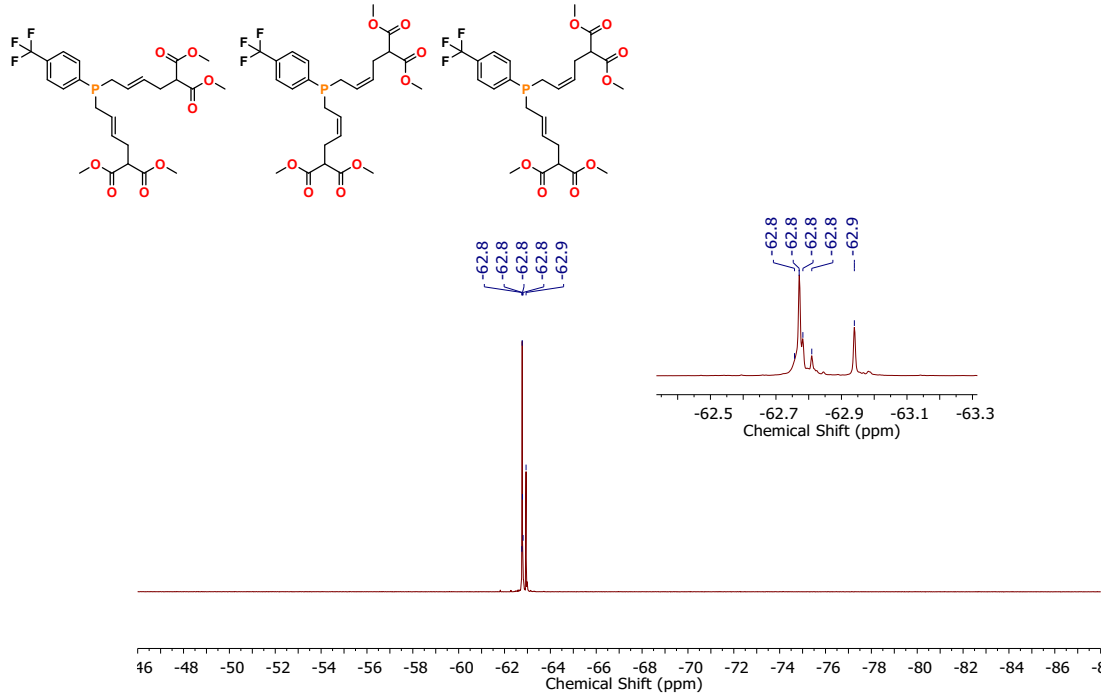

Figure S 36: $^{19}F\{^{1}H\}$ NMR spectrum of 5d recorded in $CDCl_3$.

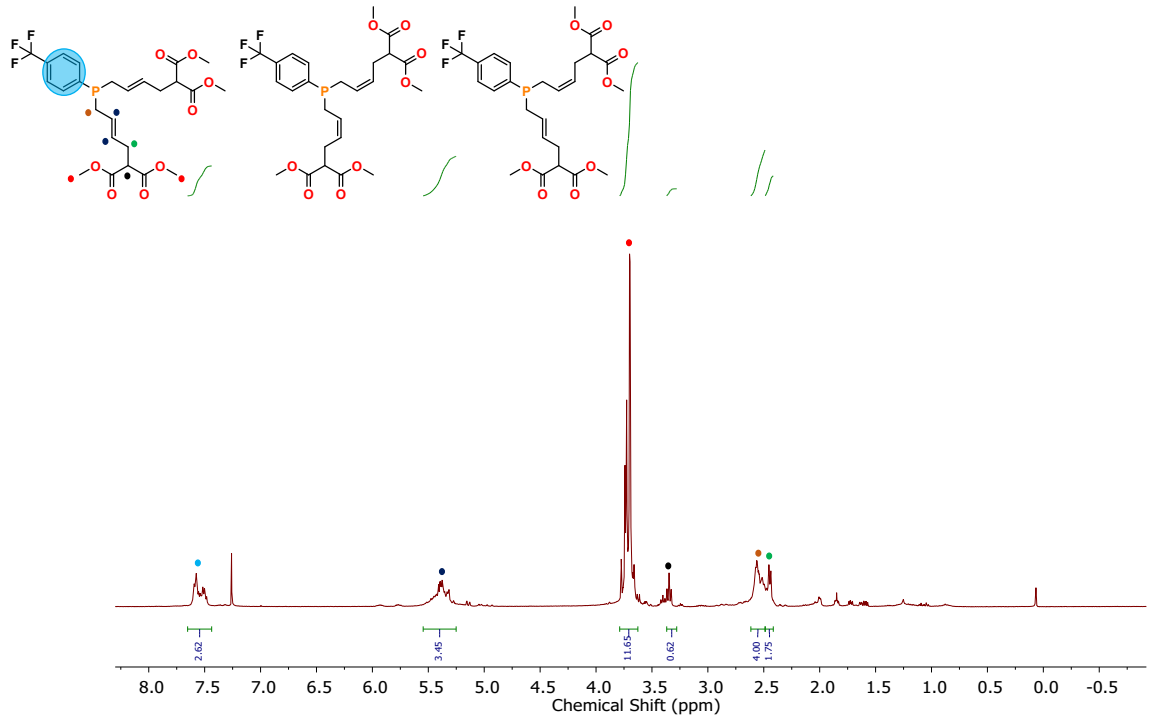

Figure S 37: ^{1}H NMR spectrum of 5d recorded in $CDCl_3$.

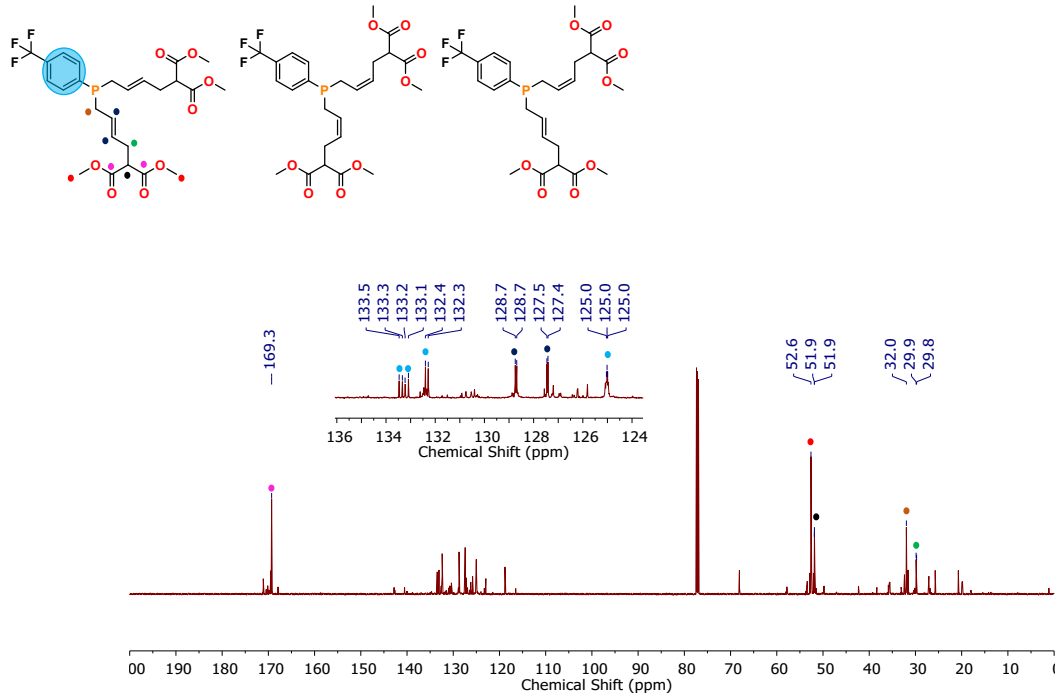

Figure S 38: $^{13}C\{^{1}H\}$ NMR spectrum of 5d recorded in $CDCl_3$.

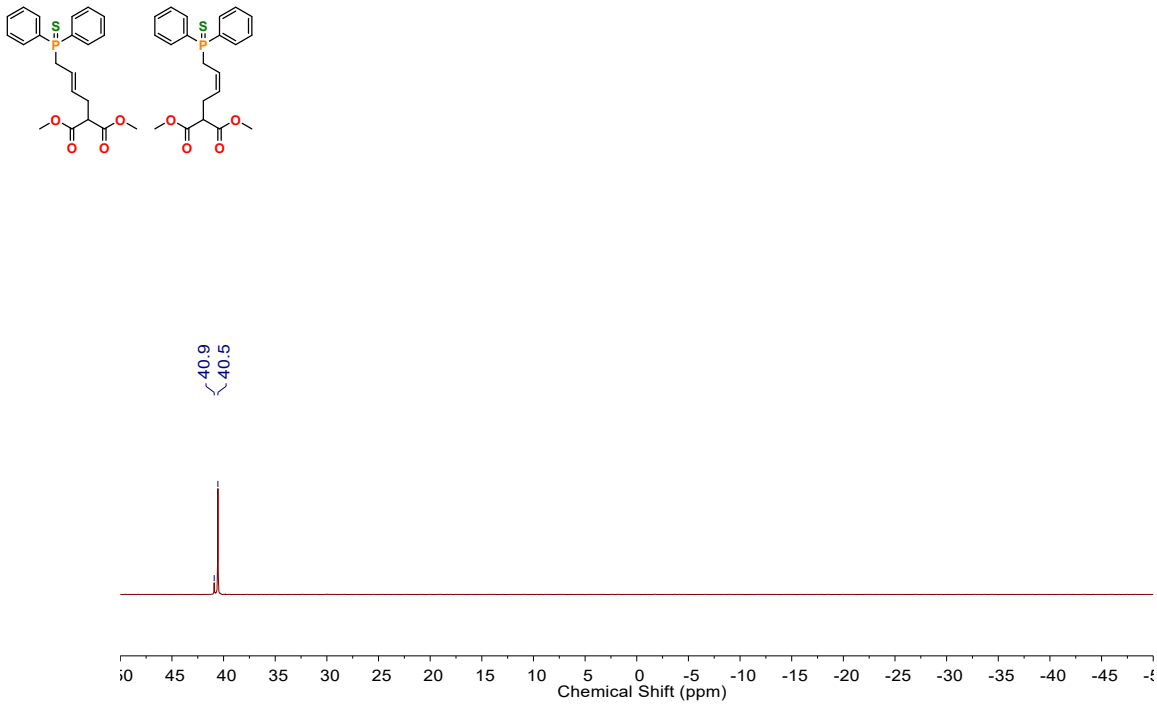

Figure S 39: $^{31}P\{^{1}H\}$ NMR spectrum of 6a recorded in $CDCl_3$.

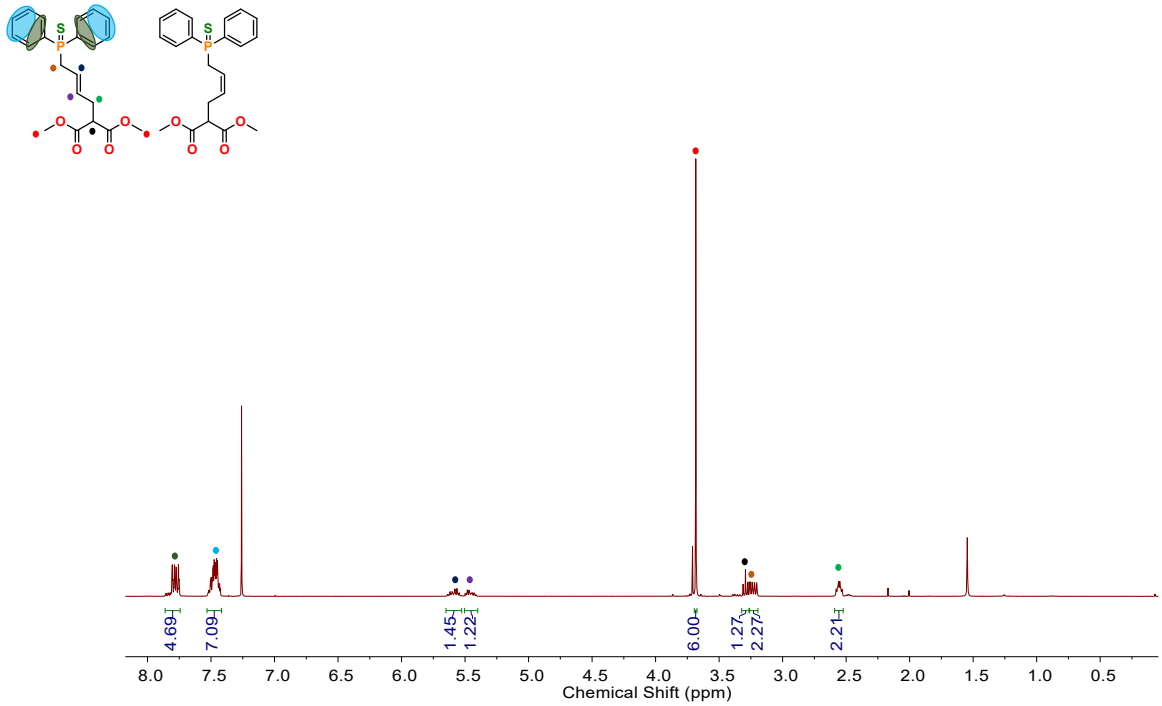

Figure S 40: ^{1}H NMR spectrum of 6a recorded in $CDCl_3$.

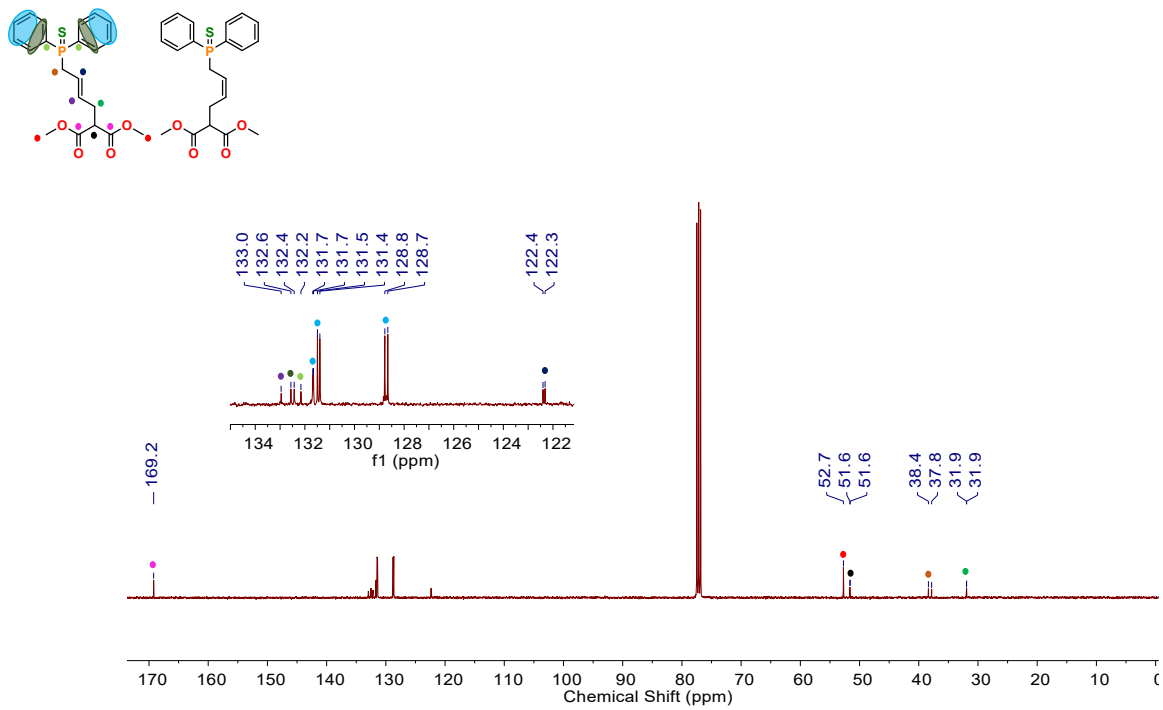

Figure S 41: $^{13}C\{^{1}H\}$ NMR spectrum of 6a recorded in $CDCl_3$.

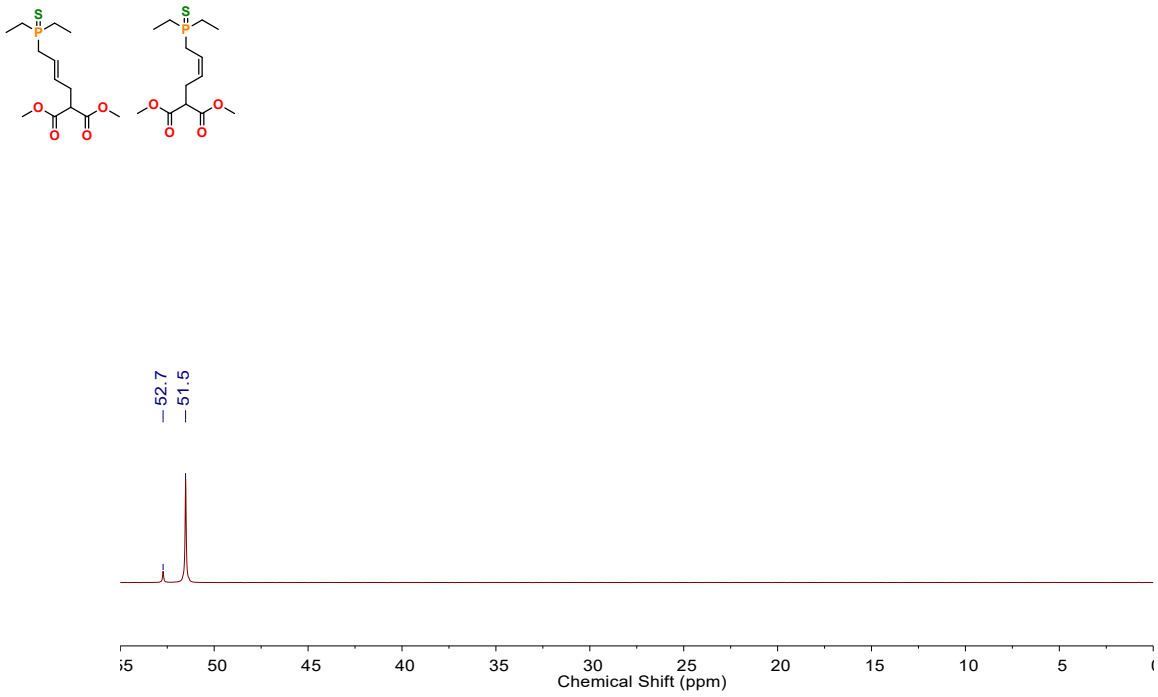

Figure S 42: $^{31}P\{^{1}H\}$ NMR spectrum of 6b recorded in $CDCl_3$.

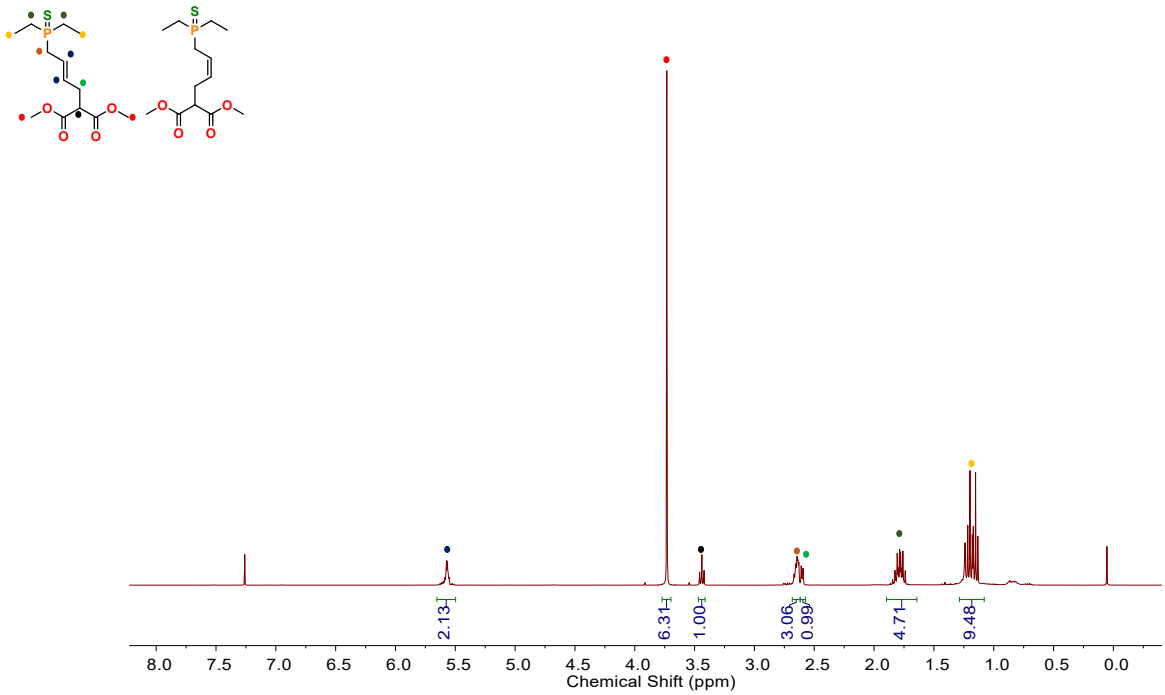

Figure S 43: ^{1}H NMR spectrum of 6b recorded in $CDCl_3$.

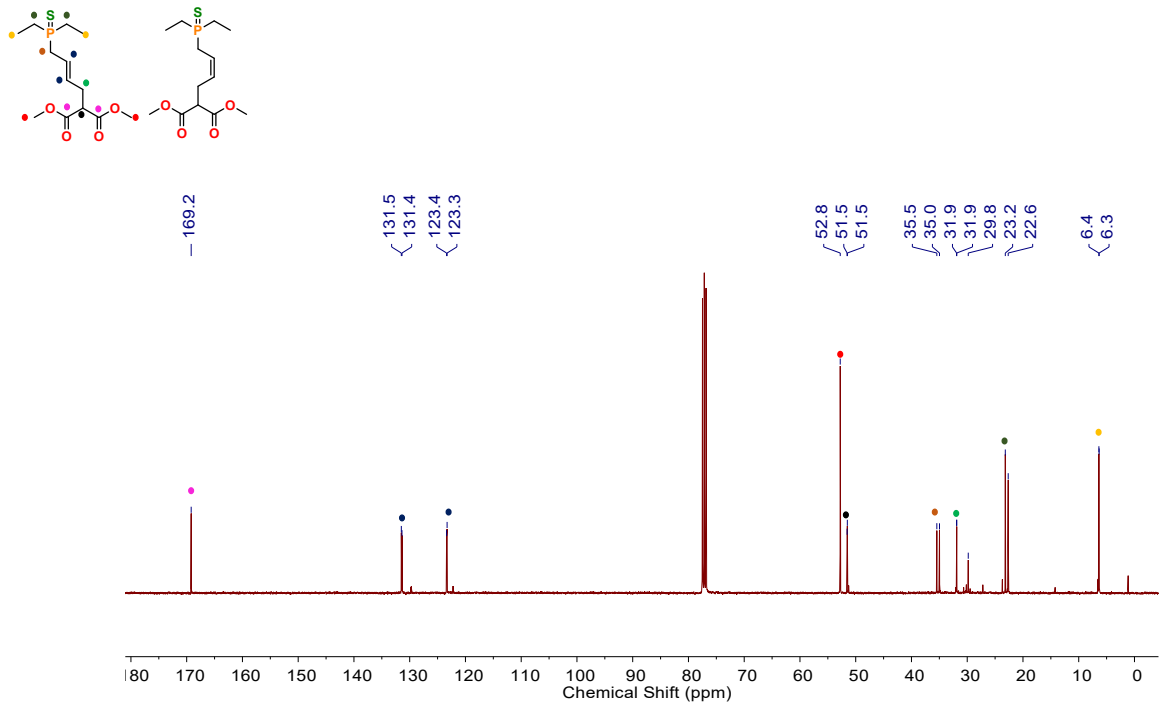

Figure S 44: $^{13}C\{^{1}H\}$ NMR spectrum of 6b recorded in $CDCl_3$.

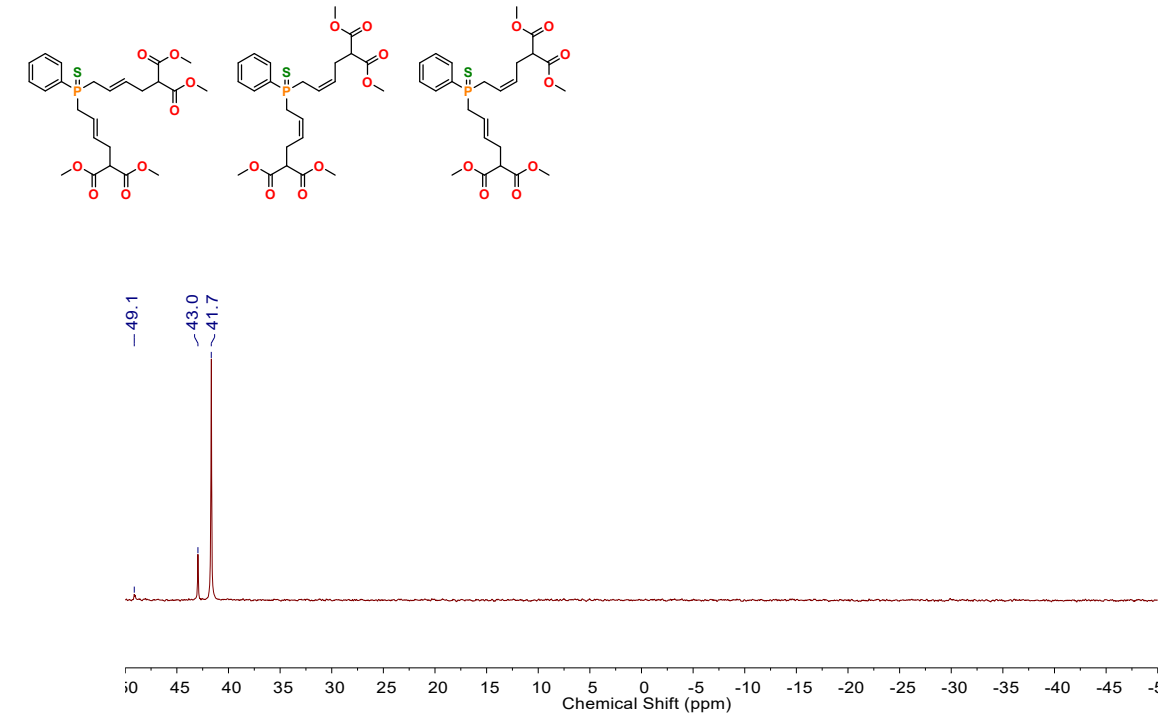

Figure S 45: $^{31}P\{^{1}H\}$ NMR spectrum of 7a recorded in $CDCl_3$.

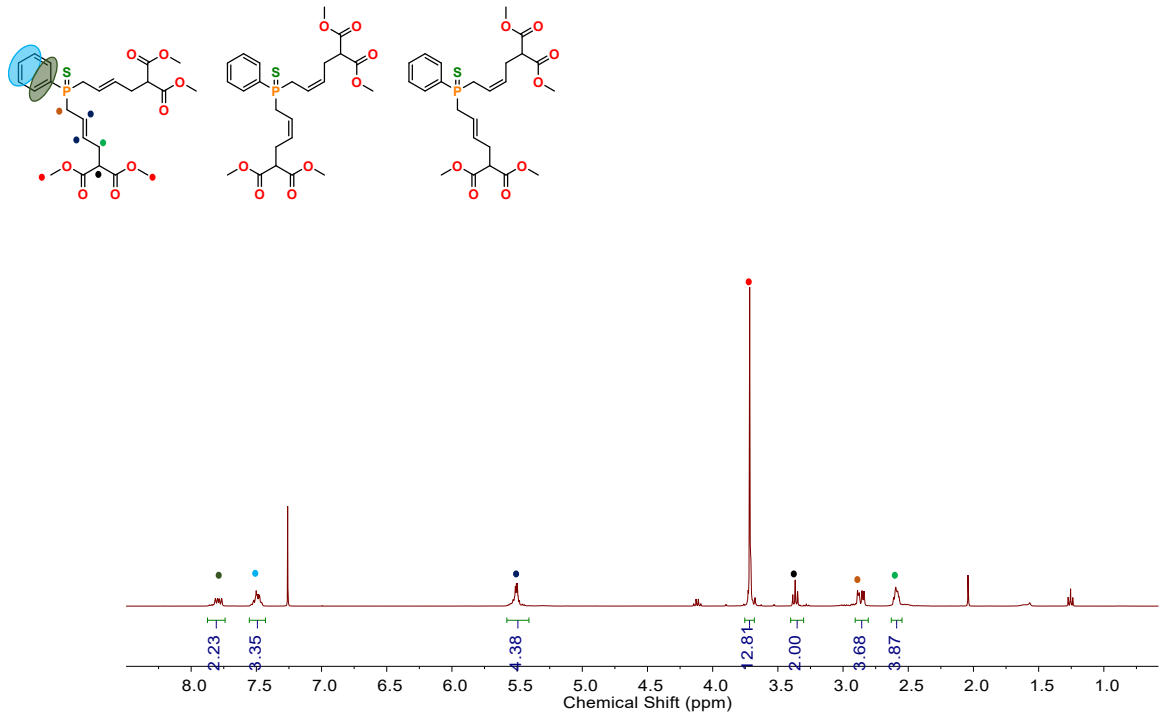

Figure S 46: ^{1}H NMR spectrum of 7a recorded in $CDCl_3$.

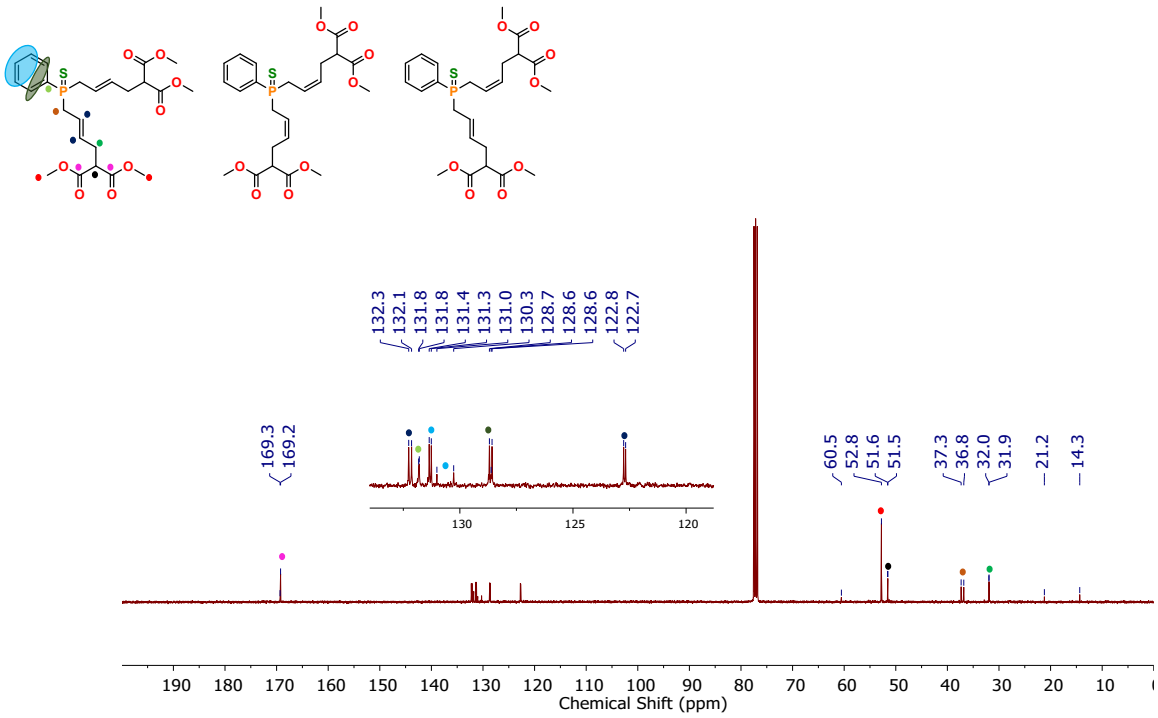

Figure S 47: $^{13}C\{^{1}H\}$ NMR spectrum of 7a recorded in $CDCl_3$.

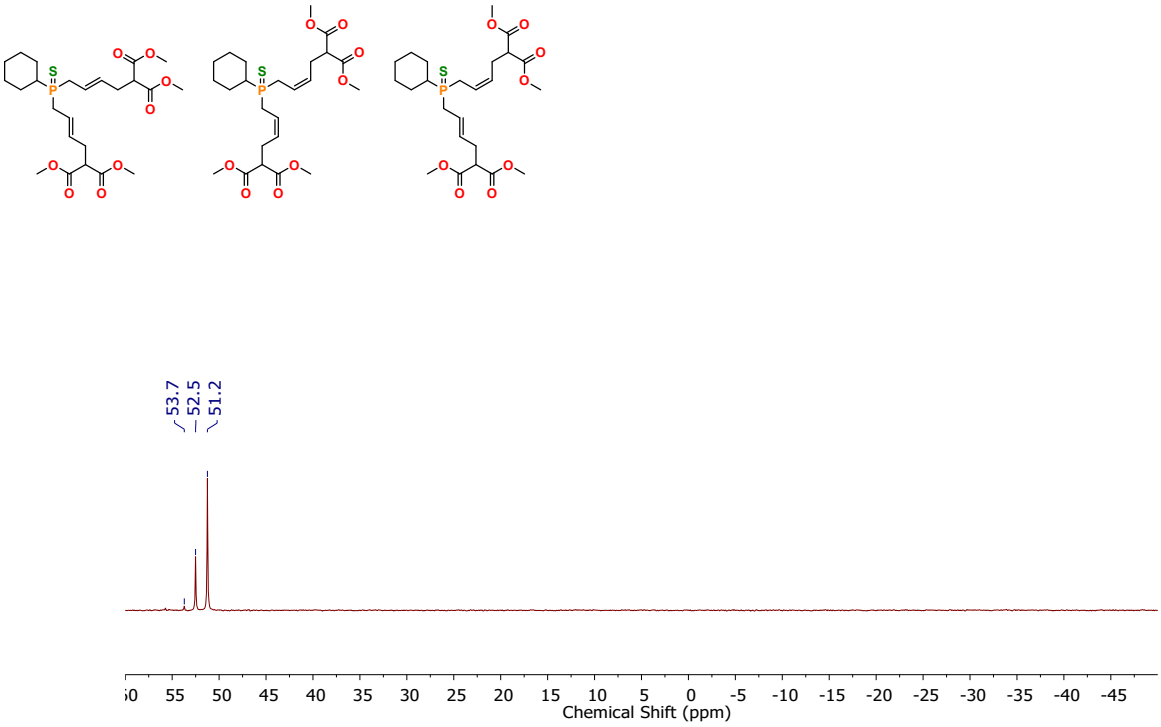

Figure S 48: $^{31}P\ \{^{1}H\}$ NMR spectrum of 7b recorded in $CDCl_3$.

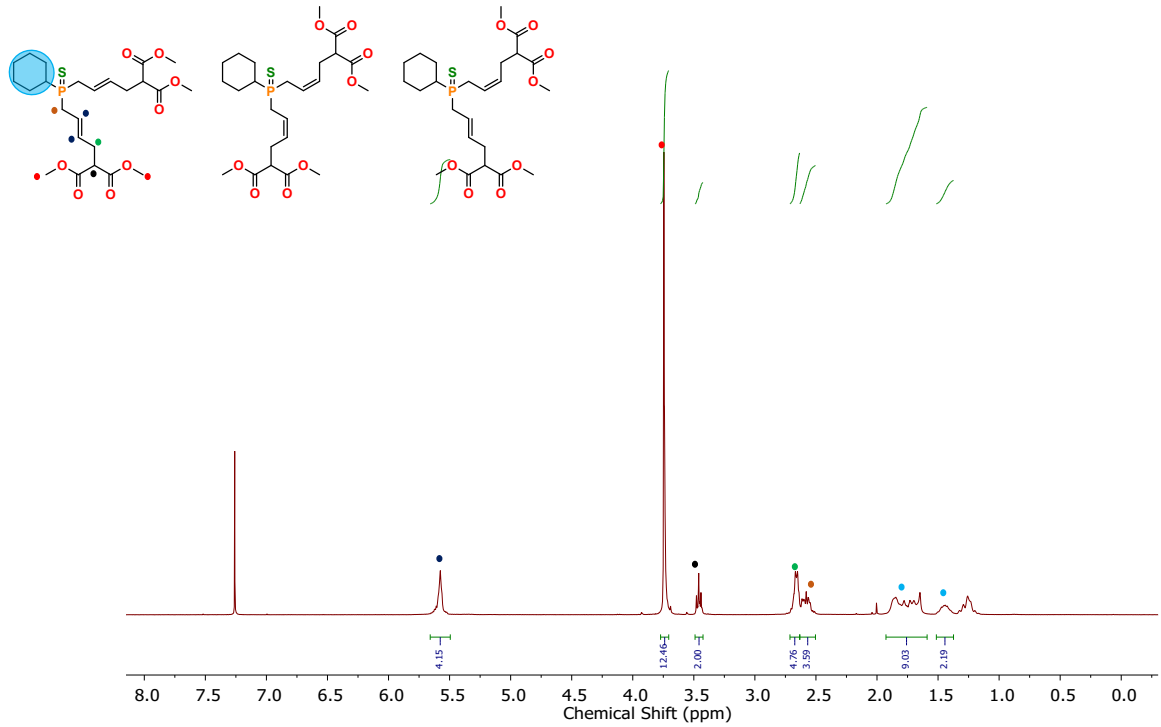

Figure S 49: ^{1}H NMR spectrum of 7b recorded in $CDCl_3$.

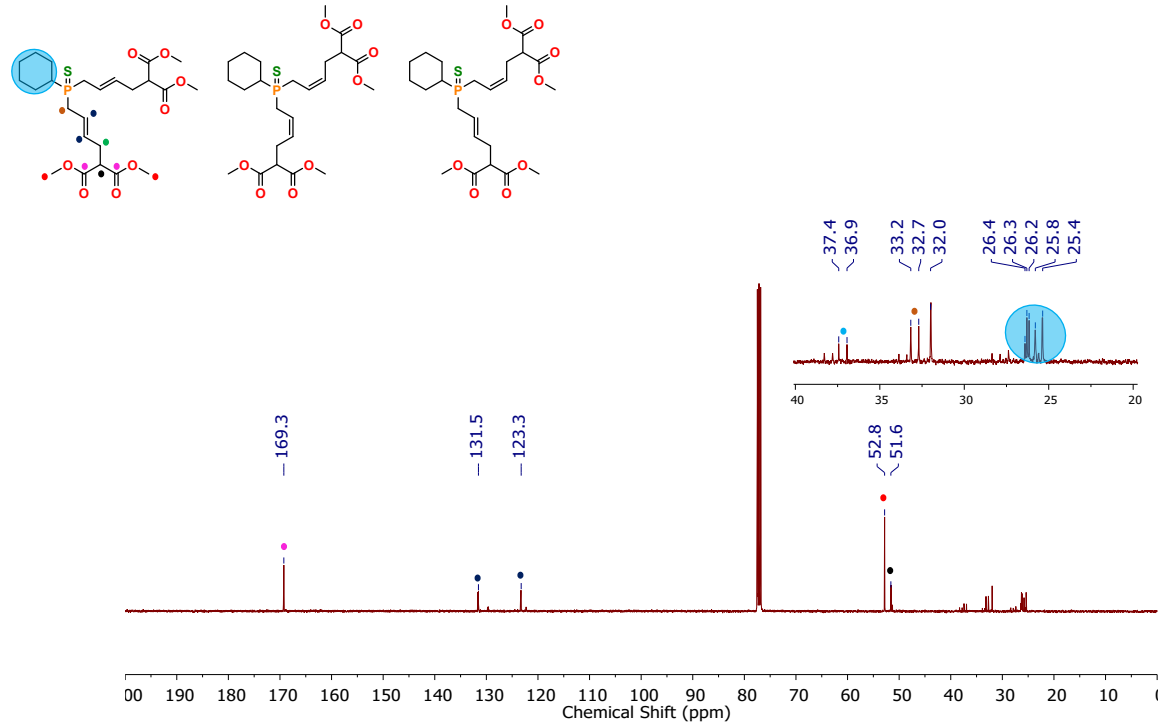

Figure S 50: $^{13}C\{^{1}H\}$ NMR spectrum of 7b recorded in $CDCl_3$.

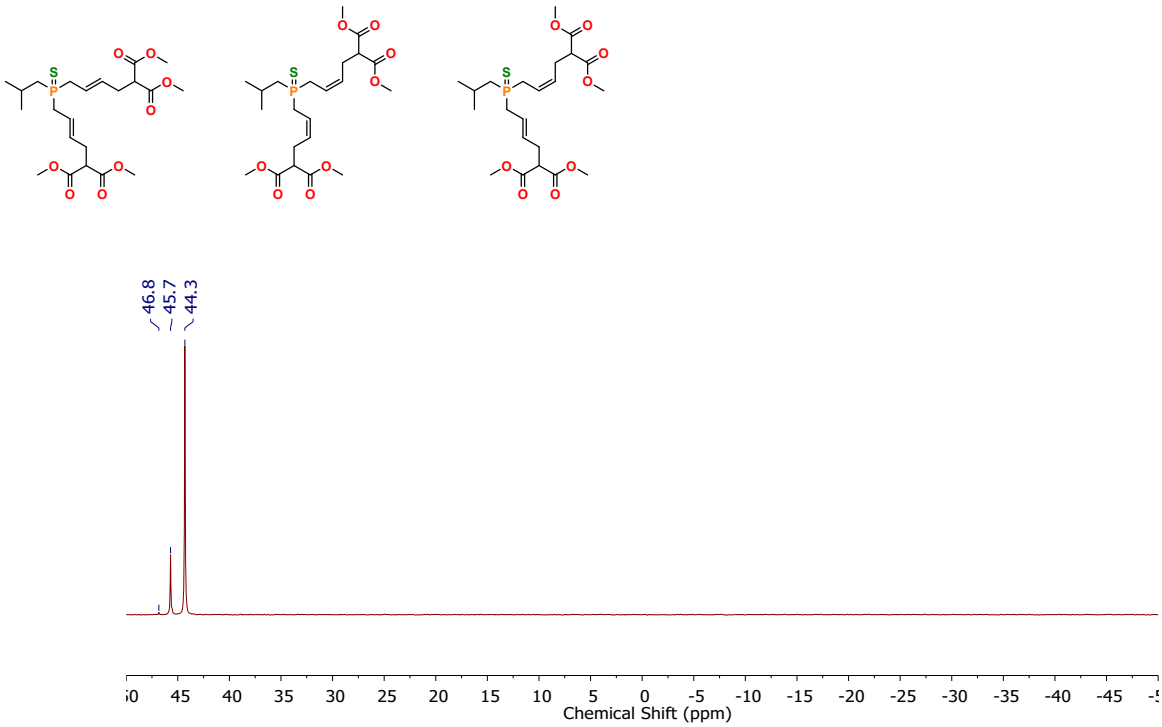

Figure S 51: $^{31}P\{^{1}H\}$ NMR spectrum of 7c recorded in $CDCl_3$.

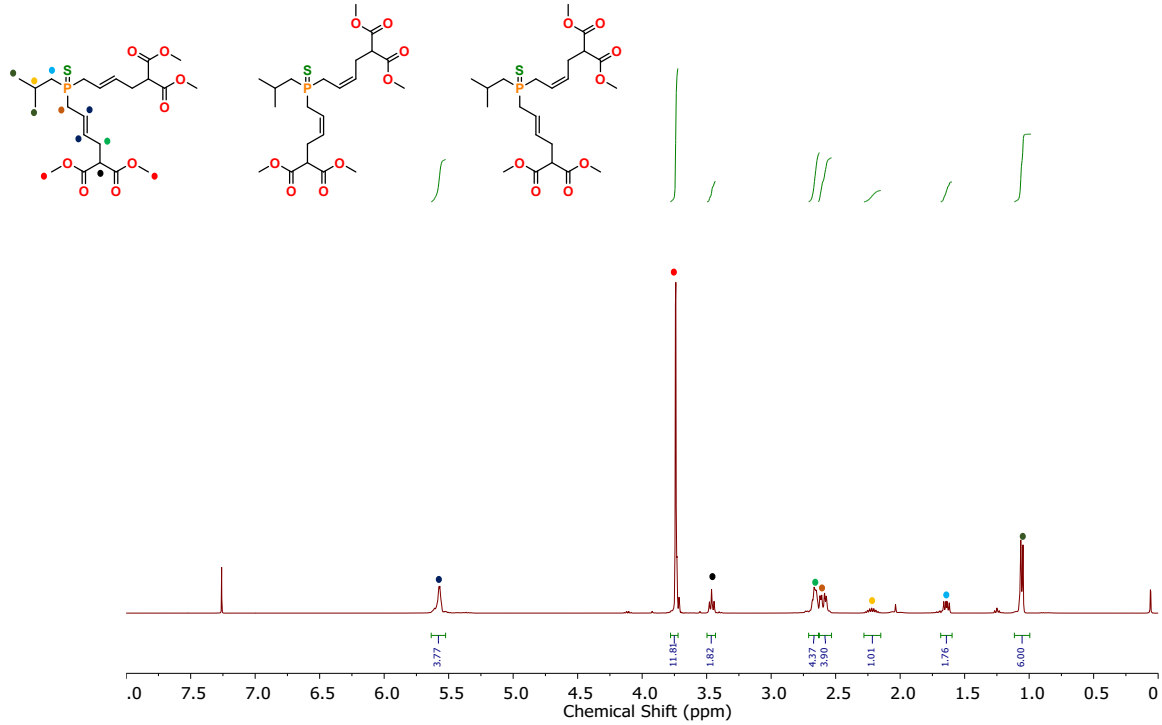

Figure S 52: ^{1}H NMR spectrum of 7c recorded in $CDCl_3$.

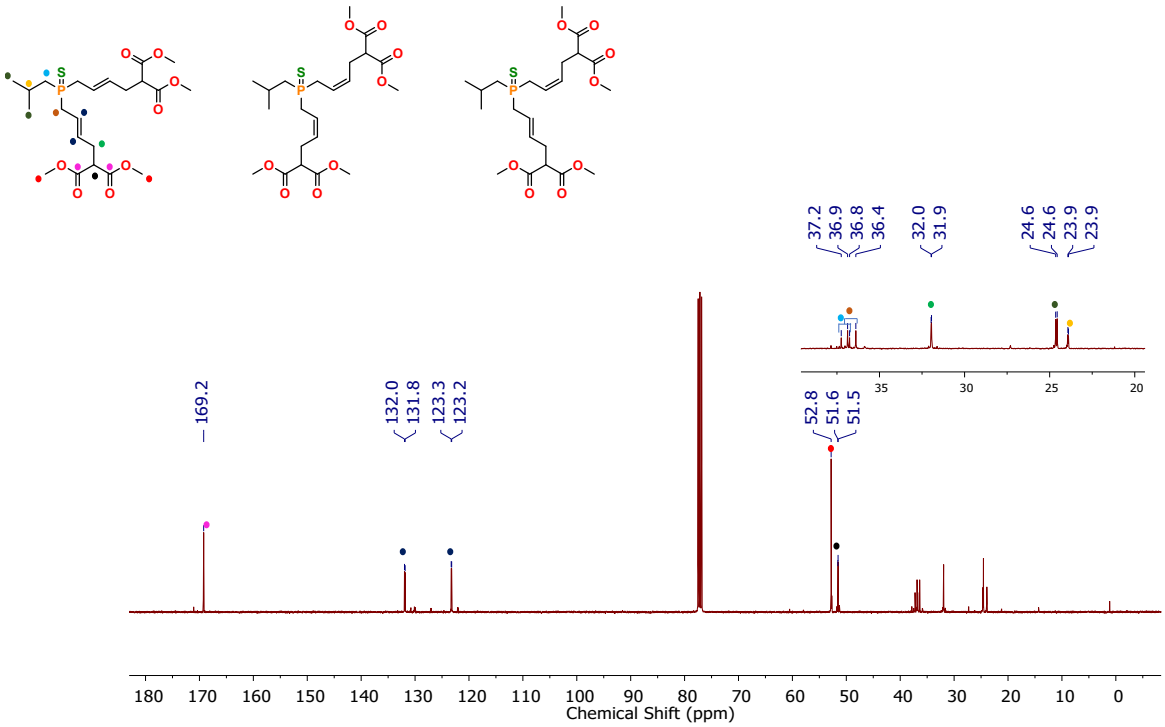

Figure S 53: $^{13}C\{^{1}H\}$ NMR spectrum of 7c recorded in $CDCl_3$.

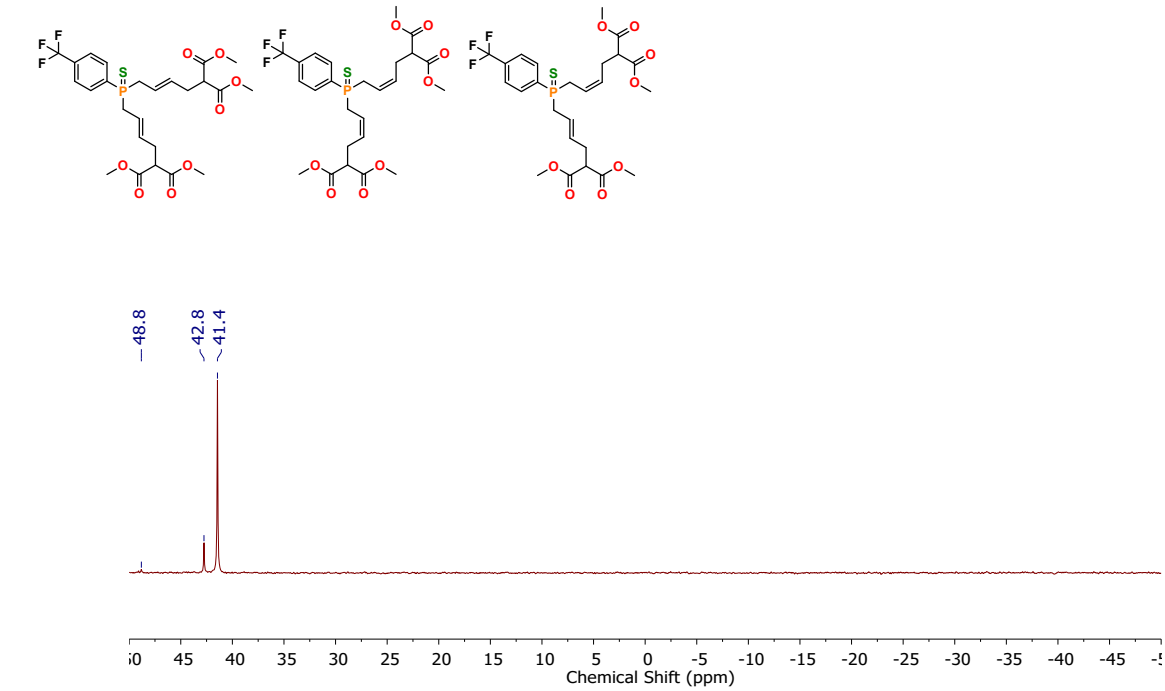

Figure S 54: $^{31}P\{^{1}H\}$ NMR spectrum of 7d recorded in $CDCl_3$.

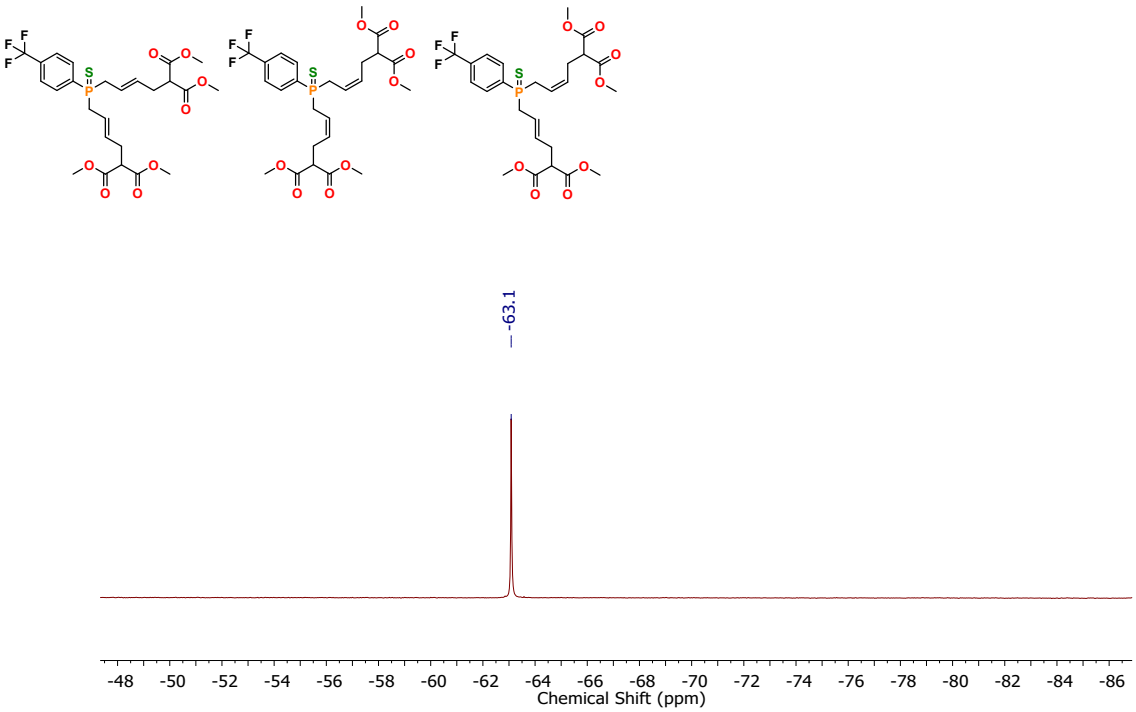

Figure S 55: $^{19}F\{^{1}H\}$ NMR spectrum of 7d recorded in $CDCl_3$.

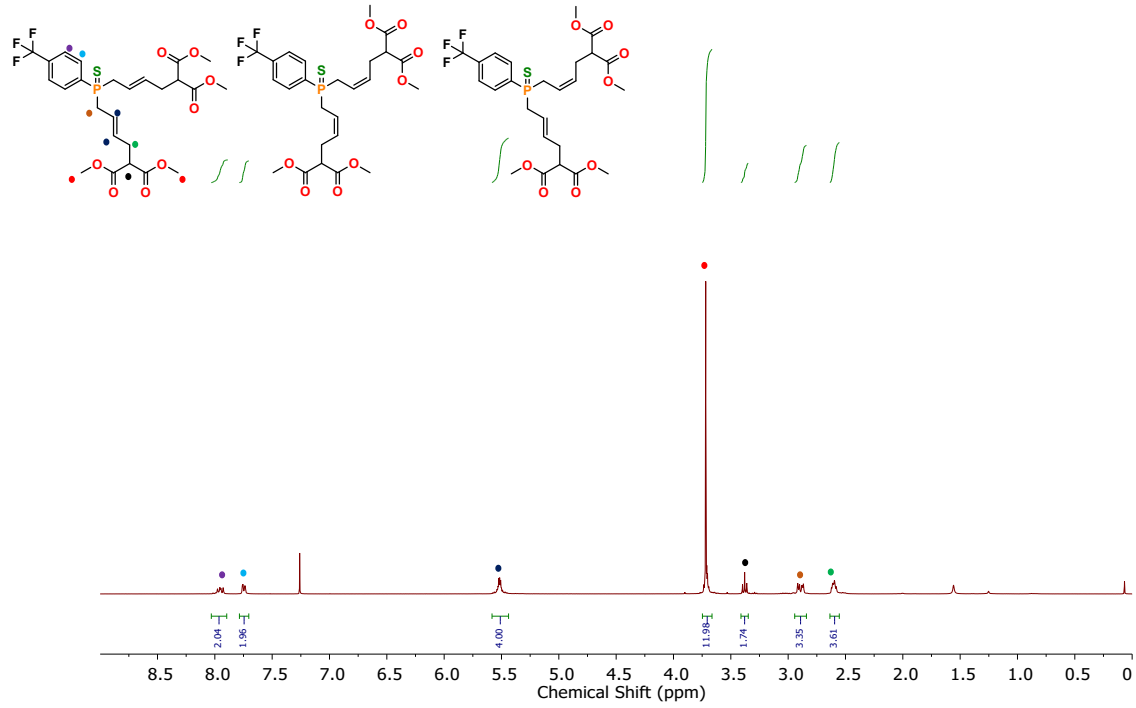

Figure S 56: ^{1}H NMR spectrum of 7d recorded in $CDCl_3$.

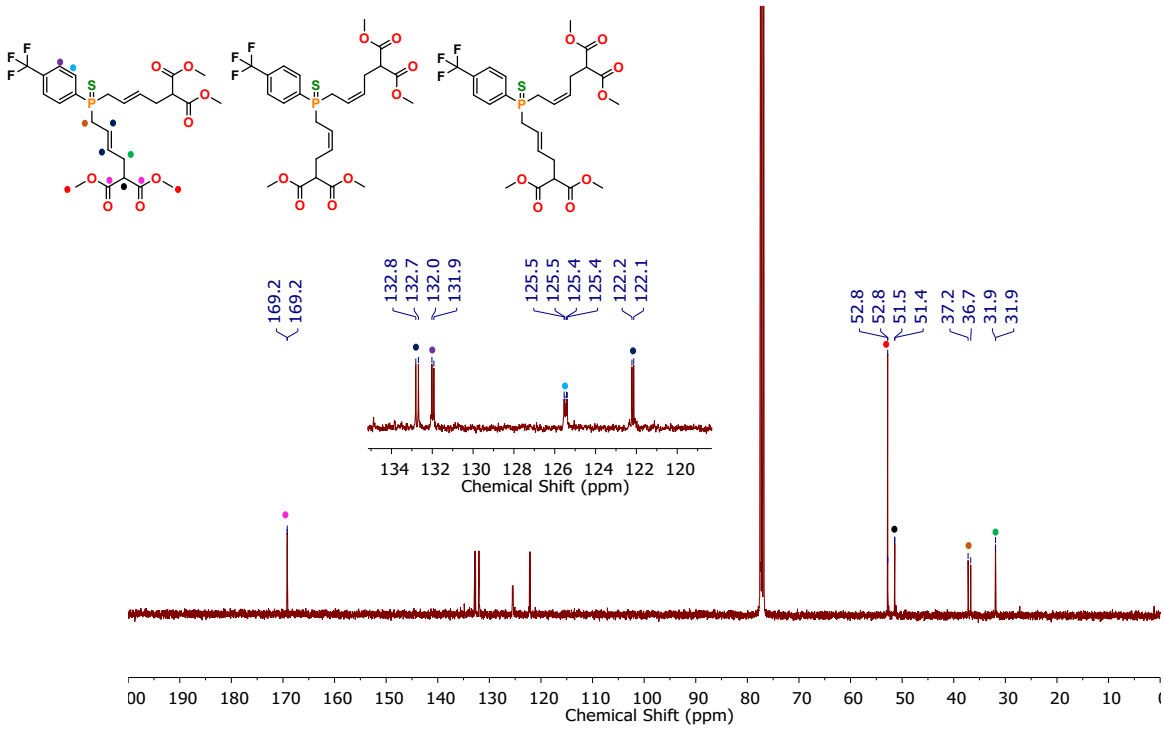

Figure S 57: $^{13}C\{^{1}H\}$ NMR spectrum of 7d recorded in $CDCl_3$.

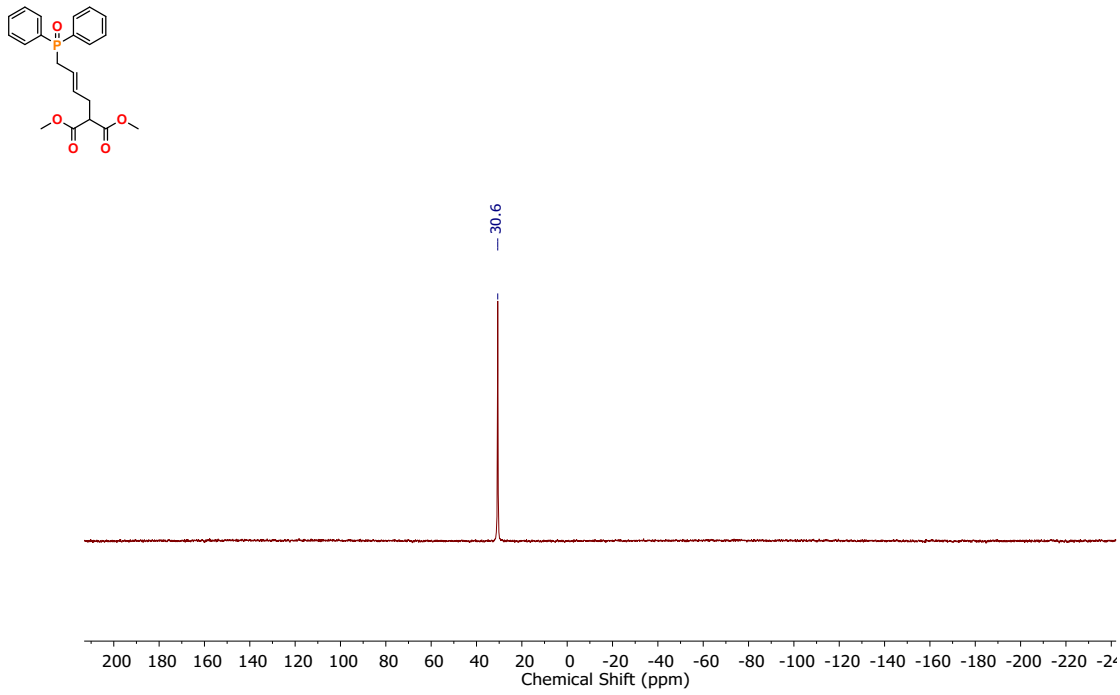

Figure S 58: $^{31}P\{^{1}H\}$ NMR spectrum of 8 recorded in $CDCl_3$.

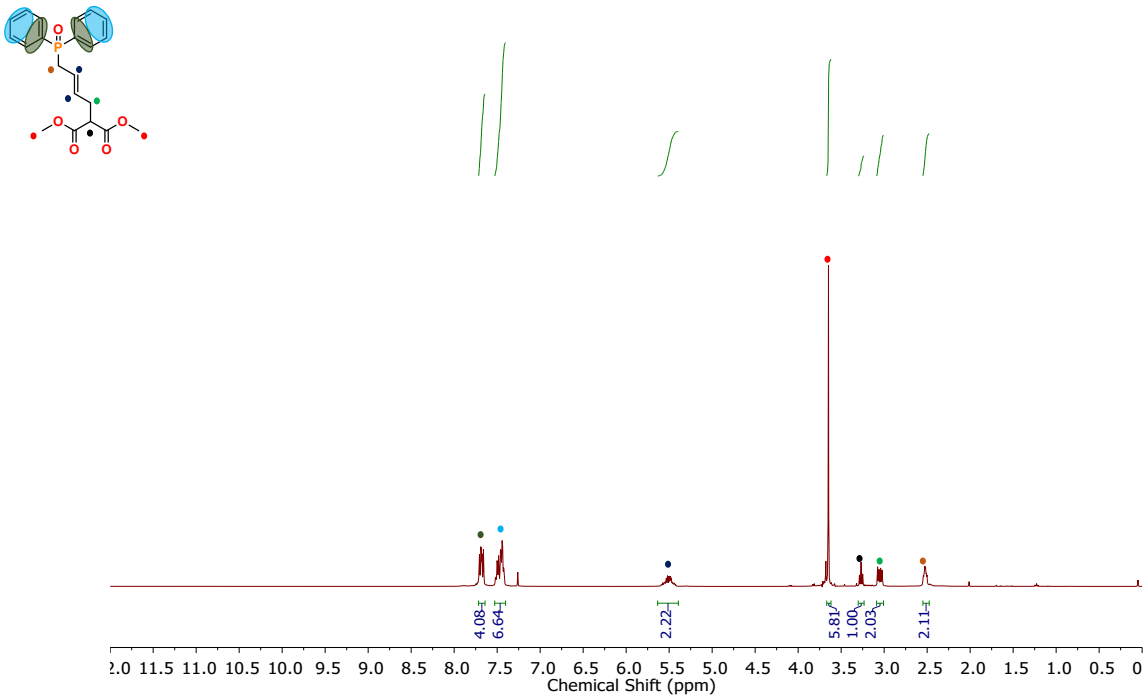

Figure S 59: ^{1}H NMR spectrum of 8 recorded in $CDCl_3$.

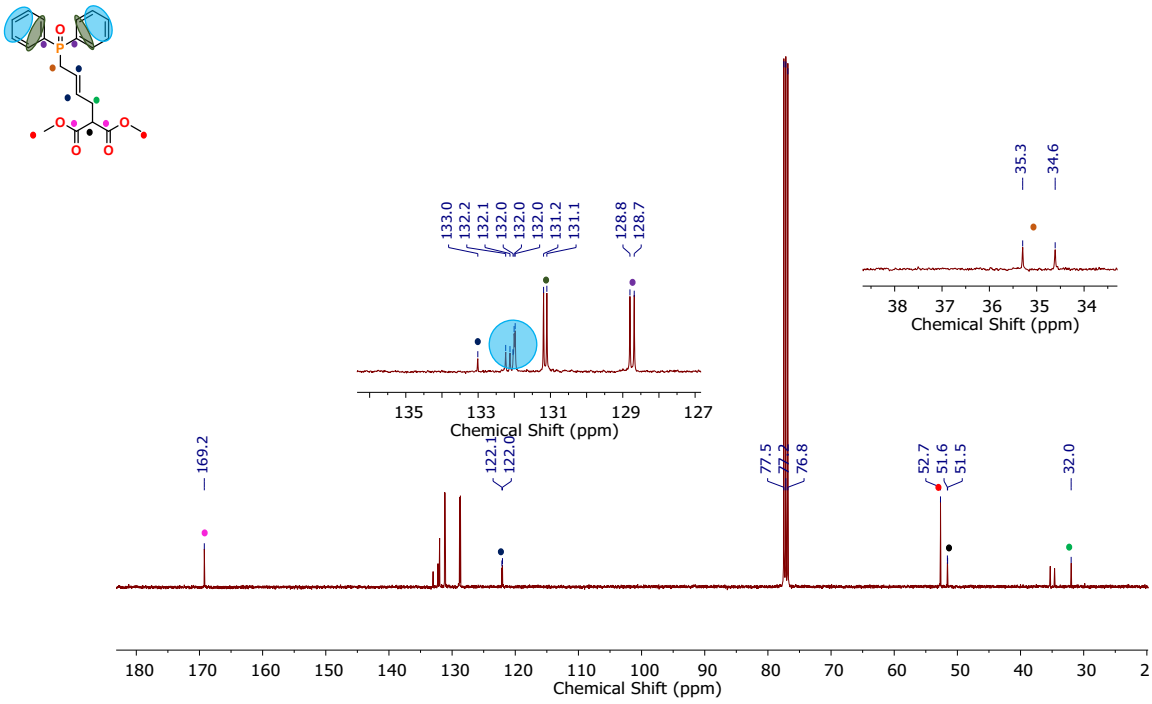

Figure S 60: $^{13}C\{^{1}H\}$ NMR spectrum of 8 recorded in $CDCl_3$.

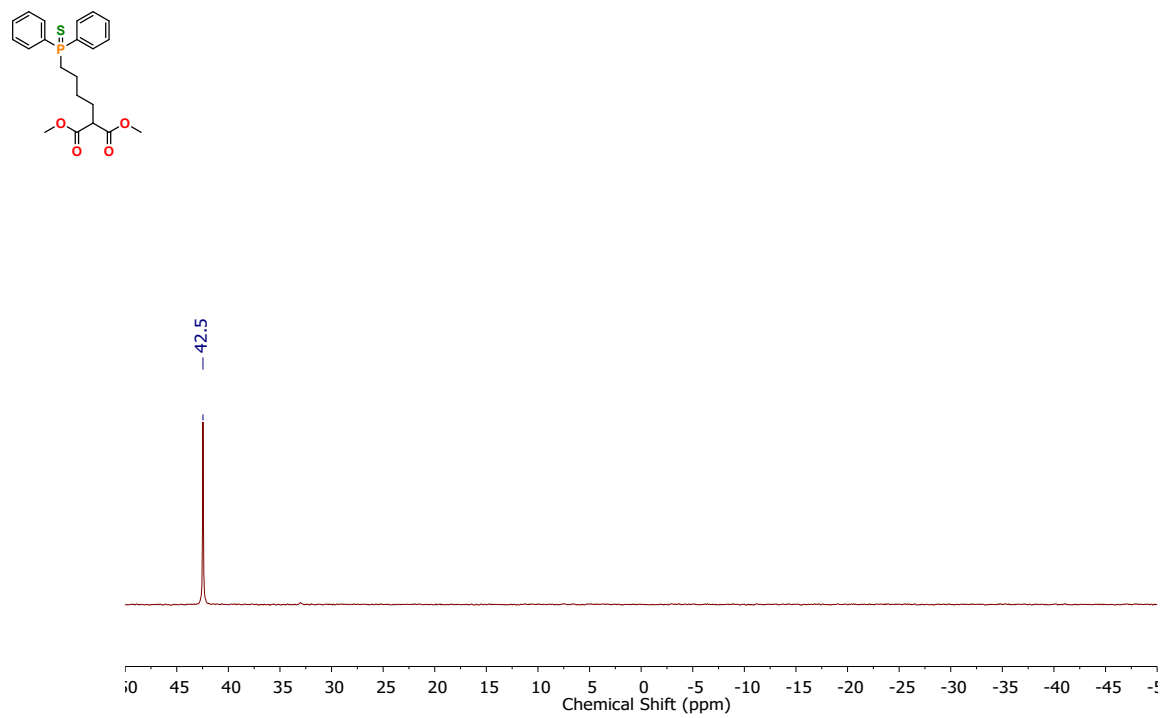

Figure S 61: $^{31}P\{^{1}H\}$ NMR spectrum of 9 recorded in $CDCl_3$.

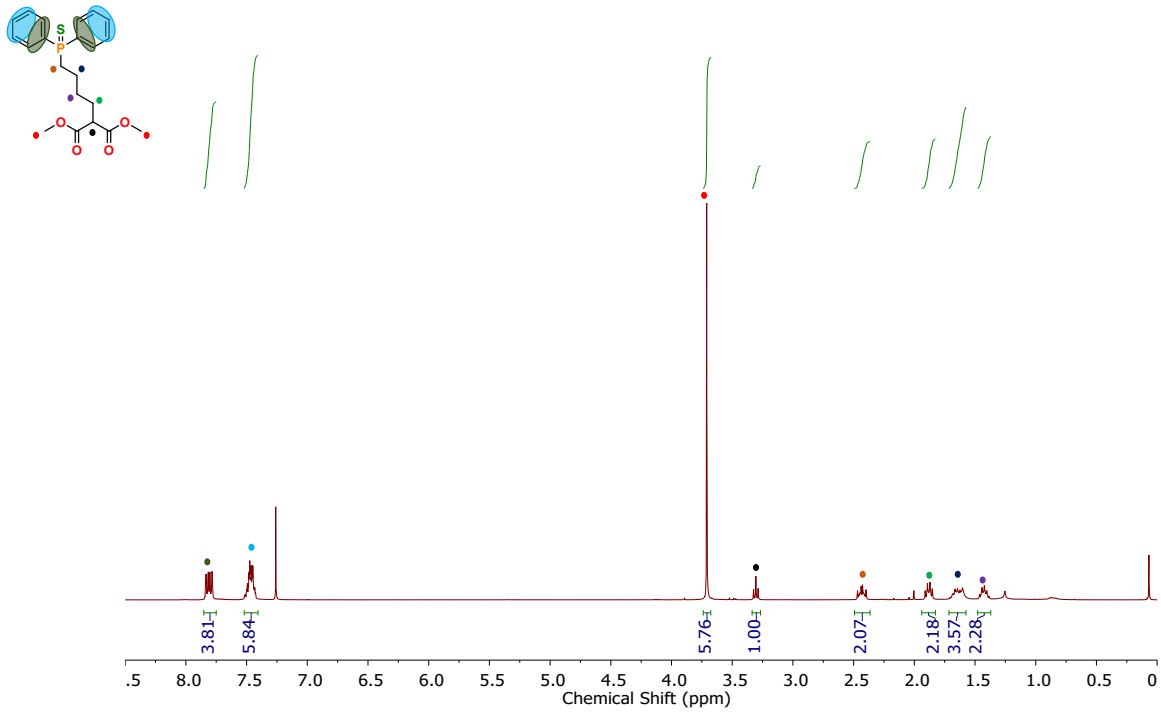

Figure S 62: ^{1}H NMR spectrum of 9 recorded in $CDCl_3$.

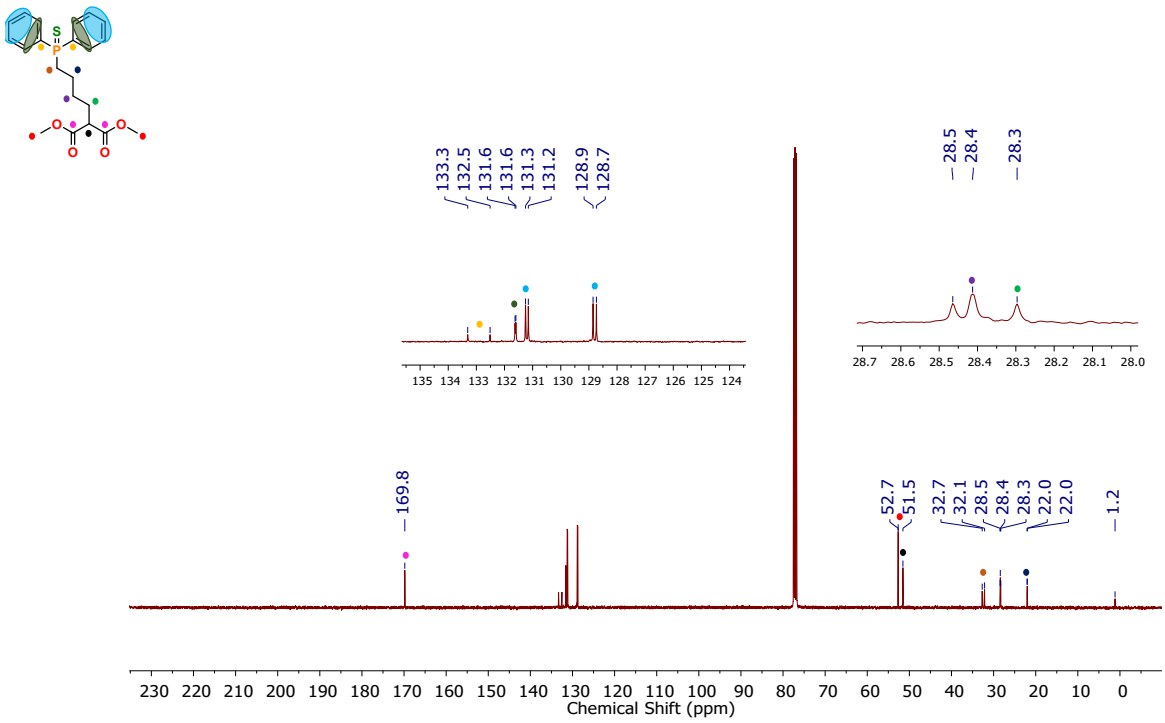

Figure S 63: $^{13}C\{^{1}H\}$ NMR spectrum of 9 recorded in $CDCl_3$.

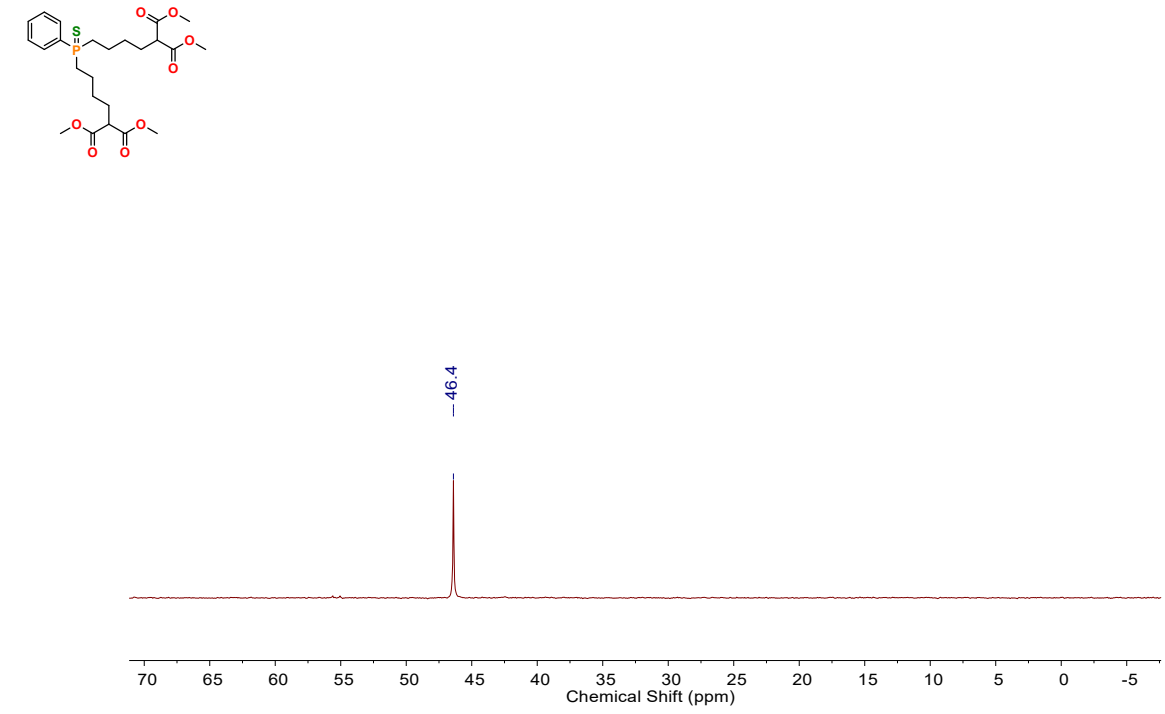

Figure S 64: $^{31}P\{^{1}H\}$ NMR spectrum of 10 recorded in $CDCl_3$.

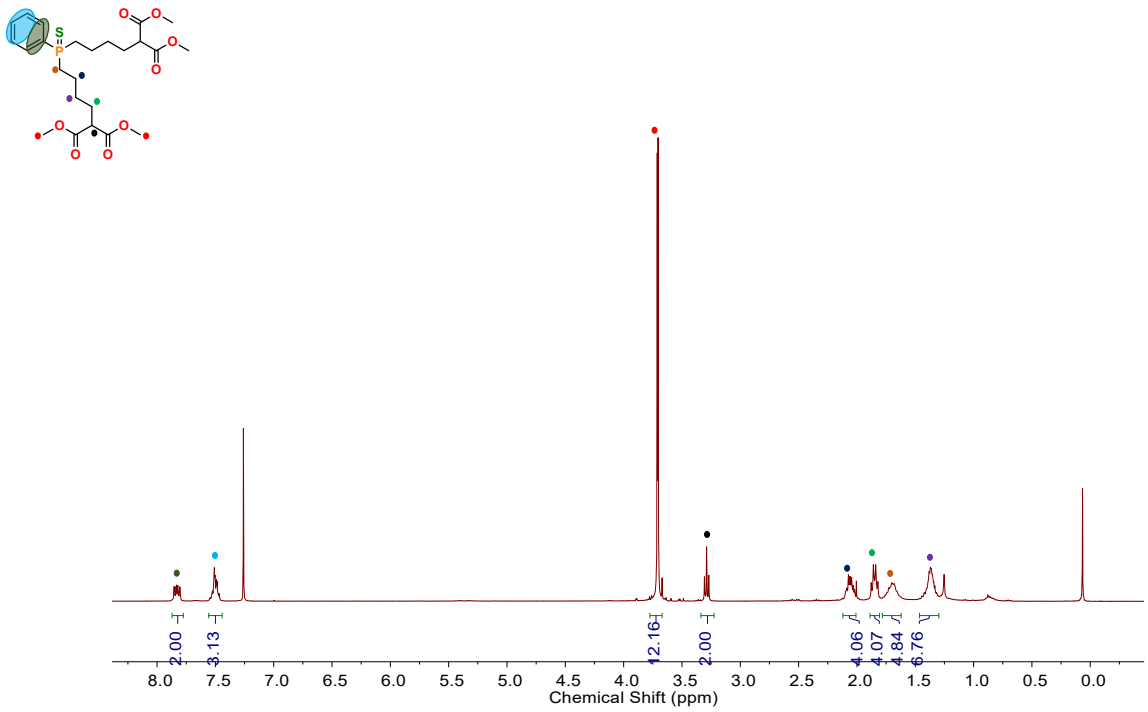

Figure S 65: ^{1}H NMR spectrum of 10 recorded in $CDCl_3$.

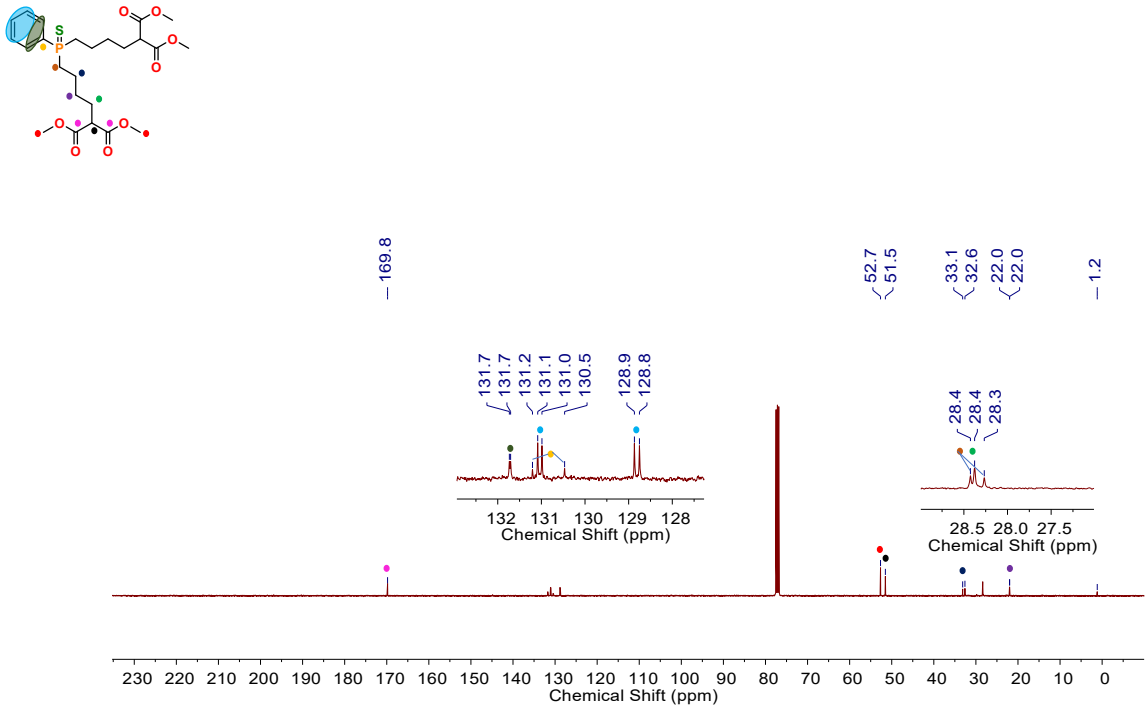

Figure S 66: $^{13}C\{^{1}H\}$ NMR spectrum of 10 recorded in $CDCl_3$.

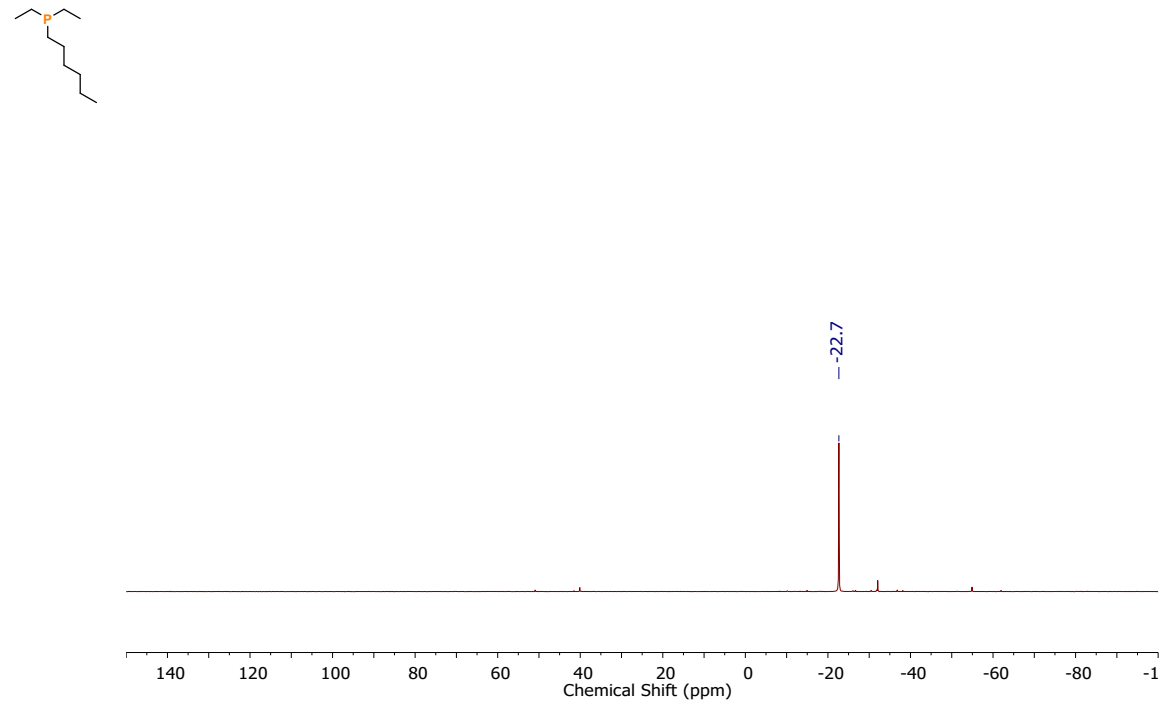

Figure S 67: $^{31}P\{^{1}H\}$ NMR spectrum of diethylhexylphosphine recorded in $CDCl_3$.

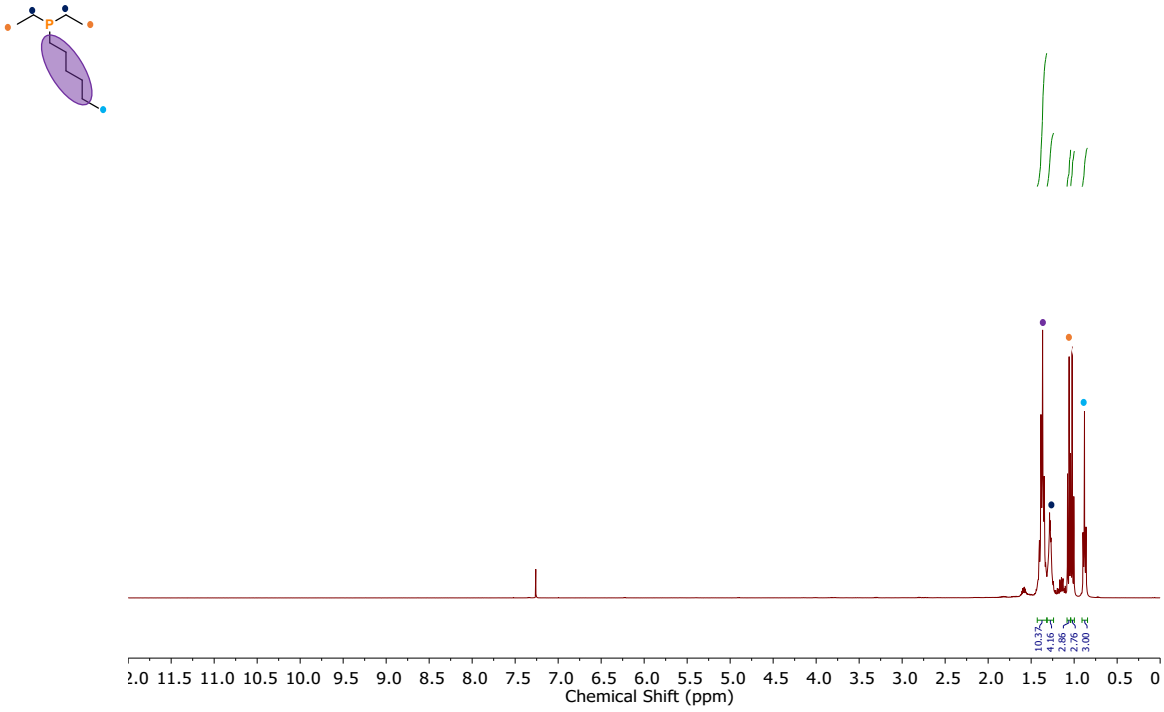

Figure S 68: ^{1}H NMR spectrum of diethylhexylphosphine recorded in $CDCl_3$.

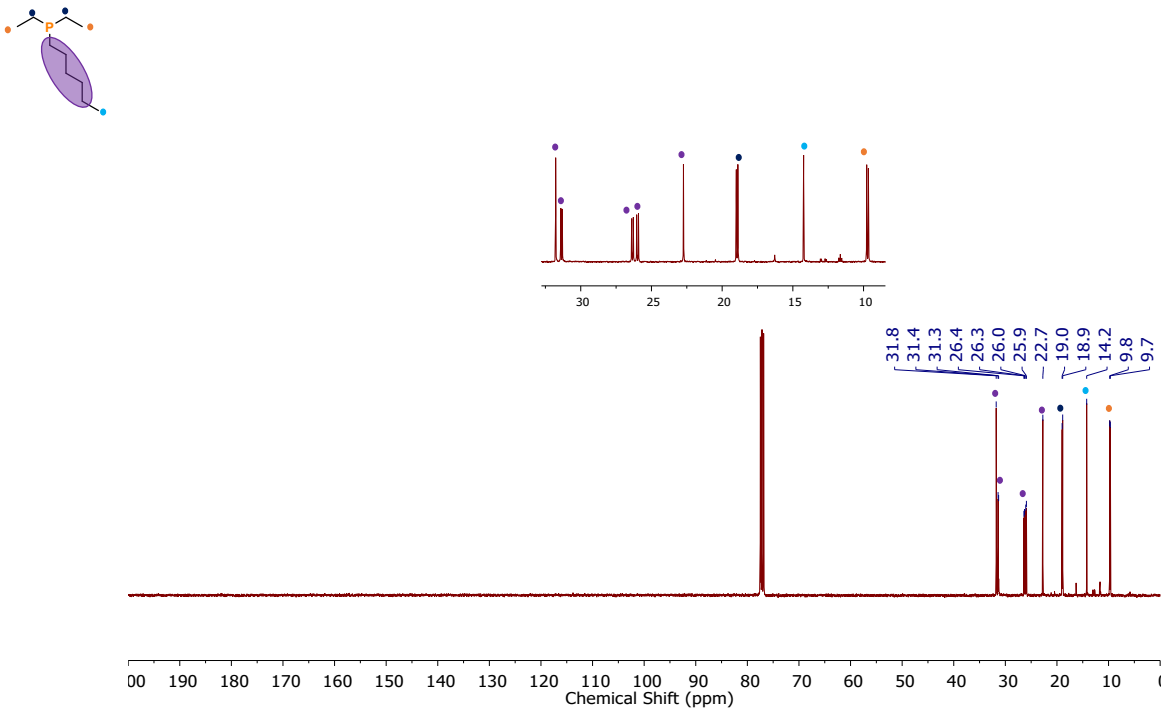

Figure S 69: $^{13}C\{^{1}H\}$ NMR spectrum of diethylhexylphosphine recorded in $CDCl_3$.

Crystallographic information

A crystal of **8** was mounted on a MiTeGen polyimide micromount with a small amount of Paratone N oil. X-ray diffraction measurements were made on a Bruker Kappa Axis Apex2 diffractometer at a temperature of 110 K. The data collection strategy involved a number of ω and φ scans which allowed for data acquisition over a range of angles, 2θ. The frame integration was performed using SAINT.[3] The resulting raw data was scaled and absorption corrected using a multi-scan averaging of symmetry equivalent data using SADABS.[4] The structure was solved by using a dual space methodology using the SHELXT program.[5] All non-hydrogen atoms were obtained from the initial solution. The hydrogen atoms were introduced at idealized positions and were allowed to ride on the parent atom. The structural model was fit to the data using full matrix least-squares based on F2. The calculated structure factors included corrections for anomalous dispersion from the usual tabulation. The structure was refined using the SHELXL 2014 program from the SHELX suite of crystallographic software.[6] Graphic plots were produced using the Mercury program.[7]

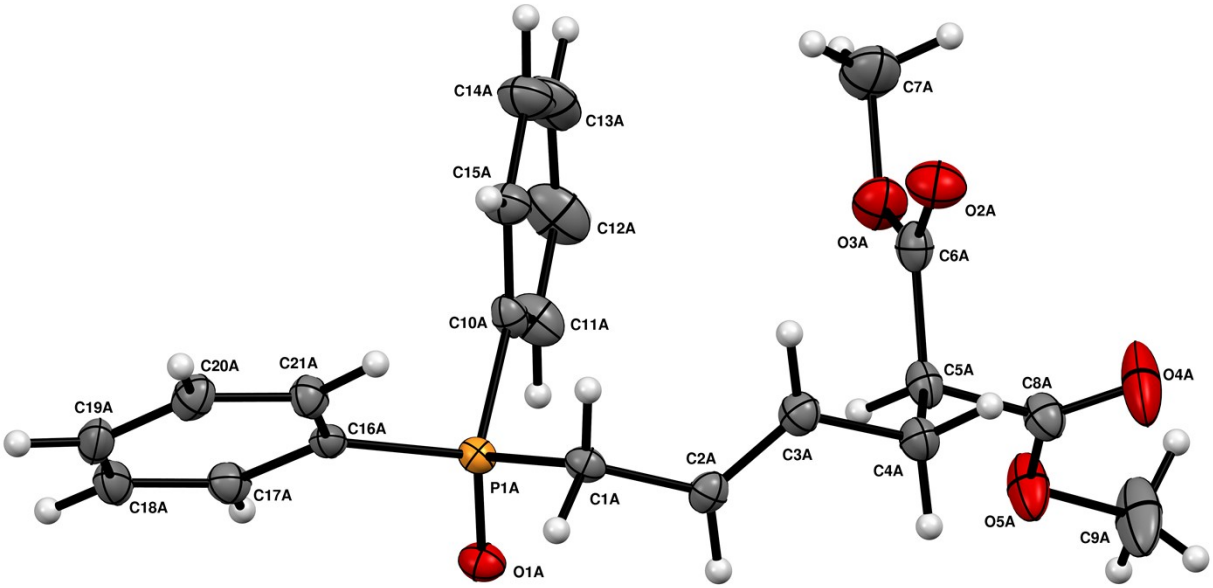

Figure S 70: ORTEP drawing of 8 molecule A showing naming and numbering scheme. Ellipsoids are at the 50% probability level and hydrogen atoms were drawn with arbitrary radii for clarity.

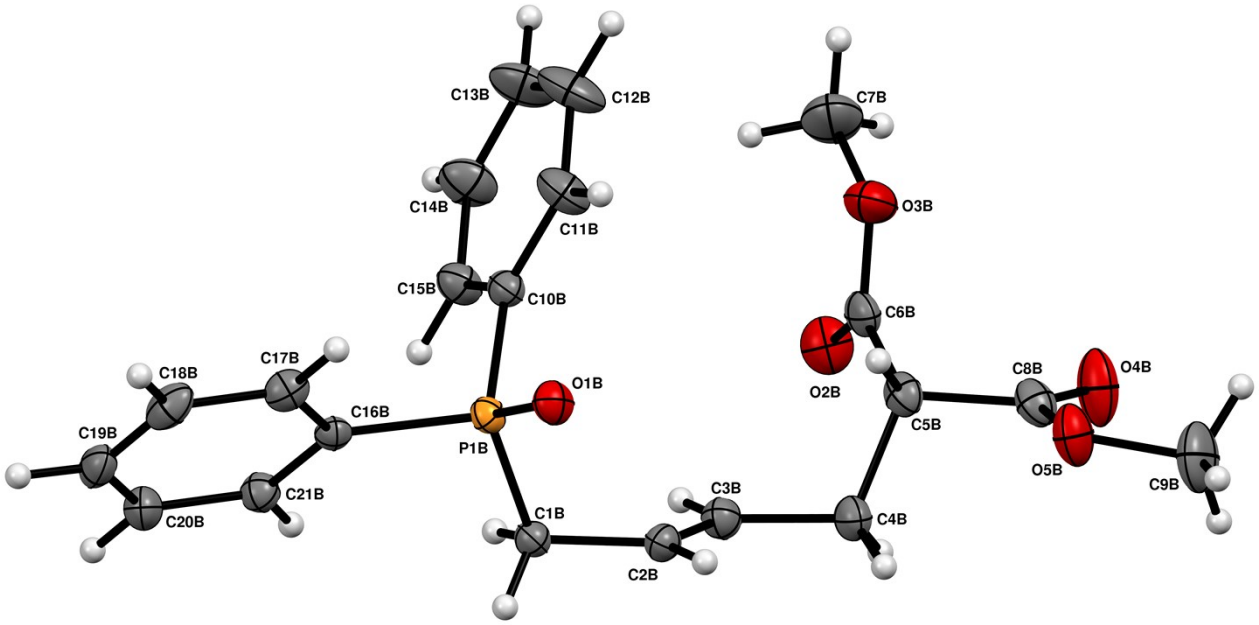

Figure S 71: ORTEP drawing of 8 molecule B showing naming and numbering scheme. Ellipsoids are at the 50% probability level and hydrogen atoms were drawn with arbitrary radii for clarity.

Table S4: Summary of Crystal Data for 8.

Formula	$C_{21}H_{23}O_5P$
Formula Weight (*g/mol*)	386.36
Crystal Dimensions (*mm*)	0.347 × 0.105 × 0.080
Crystal Color and Habit	colourless prism
Crystal System	triclinic
Space Group	P -1
Temperature, K	110
a, Å	11.3445(14)
b, Å	13.716(3)
c, Å	14.665(2)
α,°	66.288(6)
β,°	81.061(6)
γ,°	81.653(6)
V, Å^3	2055.2(6)
Number of reflections to determine final unit cell	9271
Min and Max 2θ for cell determination, °	5.0, 53.38
Z	4
F(000)	816
ρ (*g/cm*)	1.249
λ, Å, (MoKα)	0.71073
μ, (*cm^{-1}*)	0.161
Number of reflections measured	8643
Unique reflections measured	8643
R_{merge}	0.0703
Number of reflections included in refinement	8643
Number of parameters in least-squares	627
R_1	0.0443
wR_2	0.0988
R_1 (all data)	0.0698
wR_2 (all data)	0.1067
GOF	1.071
Min & Max peak heights on final ΔF Map (*e$^-$*/Å)	-0.396, 0.323

$R_1 = \Sigma(|F_o| - |F_c|) / \Sigma F_o$

GOF = [Σ(w(F_o^2 - F_c^2)^2) / (No. of reflns. - No. of params.)]^{½}

References

1 M. Kasha, *J. Opt. Soc. Am.*, 1948, **38**, 929 – 934.

2 S. L. Murov, I. Carmichael and G. L. Hug, in *Handbook of Photochemistry*, 2nd ed, CRC Press, New York, 1993, Section 14, pp. 314–324.

3. Bruker, SAINT (8.34A), Bruker AXS Inc., Madison, Wisconsin, USA, 2013.

4. Bruker SADABS-2012/1, Bruker AXS Inc., Madison, Wisconsin, USA, 2012.

5. G. M. Sheldrick, *Acta Cryst.*, 2015, A**71**, 3 – 8.

6. G. M. Sheldrick, *Acta Cryst.*, 2015, C**71**, 3 – 8.

7. C. F. Macrae, I. J. Bruno, J. A. Chisholm, P. R. Edington, P. McCabe, E. Pidcock, L. Rodriguez-Monge, R. Taylor, J. van de Streek, and P. A. Wood, *J. Appl. Cryst.*, 2008, **41**, 466 – 470.